

E_{1g} model of superconducting UPt_3

K. A. Park and Robert Joynt

Department of Physics and Applied Superconductivity Center

University of Wisconsin-Madison

1150 University Avenue

Madison, Wisconsin 53706

(October 16, 2018)

Abstract

The phase diagram of superconducting UPt_3 is explained in a Ginzburg-Landau theory starting from the hypothesis that the order parameter is a pseudo-spin singlet which transforms according to the E_{1g} representation of the D_{6h} point group. We show how to compute the positions of the phase boundaries both when the applied field is in the basal plane and when it is along the c-axis. The experimental phase diagrams as determined by longitudinal sound velocity data can be fit using a single set of parameters. In particular the crossing of the upper critical field curves for the two field directions and the apparent isotropy of the phase diagram are reproduced. The former is a result of the magnetic properties of UPt_3 and their contribution to the free energy in the superconducting state. The latter is a consequence of an approximate particle-hole symmetry. Finally we extend the theory to finite pressure and show that, in contrast to other models, the E_{1g} model explains the observed pressure dependence of the phase boundaries.

PACS Nos. 74.70.Tx, 74.25.Dw, 74.20.De.

arXiv:cond-mat/9506112v1 23 Jun 1995

Typeset using REVTeX

I. INTRODUCTION

Currently, there is a great deal of discussion about the nature of the superconducting heavy-fermion compounds, especially UPt₃. Much of this discussion has centered on the unusual nature of the superconducting state. Experiments to map out the phase diagram of UPt₃ in the field-temperature ($H - T$) plane using both specific heat [1,2] and longitudinal sound absorption [3,4] and velocity [5,6] have revealed multiple superconducting phases. In particular these measurements show that two superconducting phases exist even at zero field, as was predicted [7] by an analysis of the free energy for a two-component order parameter in the presence of antiferromagnetism. [8] The resulting Ginzburg-Landau (G-L) theory makes additional predictions - e. g. the kink in the upper critical field when the field is in the basal plane. [9,10] In these theories, the order parameter transforms as one of the irreducible representations of the D_{6h} point group of the crystal. either E_1 or E_2 . [12,11]

Further evidence about the superconducting state of UPt₃ comes from measurements of ultrasound [13,14] and heat conduction. [15] These experiments suggest that there are point nodes in the superconducting gap function where the Fermi surface intersects the line $k_x = k_y = 0$ and line nodes where the Fermi surface intersects the $k_z = 0$ or $k_z = \pi/c$ planes. This is evidence for a d-wave E_{1g} order parameter which transforms like $(k_x k_z, k_y k_z)$. The theorem of Blount [16] states that triplet states cannot have lines of nodes when spin-orbit coupling is taken into account. The theorem assumes that no symmetries are present other than the crystal point group symmetries. It has been argued that other symmetries may be present in UPt₃ [17] and thus lines of nodes may be present even if the Cooper pair is a triplet. Thus the nodal pattern may not prove singlet pairing.

In spite of the success of the E_{1g} model in explaining the nodal structure of the gap function and the existence of multiple superconducting phases, certain objections have been raised regarding its suitability as a description of UPt₃. One objection is that the E_{1g} theory fails to explain the isotropy of the phase diagram, or, in other words, why the phase diagram when the field is parallel to the c-axis of the crystal appears to be similar to the phase diagram when the field is perpendicular to the c-axis. [17,18] We shall argue that there are similarities but also important differences and that the E_{1g} theory does in fact explain the phase diagram for both orientations of \mathbf{H} . The other common objection to the E_{1g} theory is that because it is a singlet theory it cannot explain why the upper critical field curve for \mathbf{H} along the c-axis and the curve for \mathbf{H} in the basal plane cross. [19] This crossing is maintained to be a characteristic of triplet theories alone. [20] By a careful analysis of the magnetic properties of UPt₃ and their contributions to the G-L free energy we will show that pseudo-spin singlet states can also produce this effect.

The plan for the rest of this paper is as follows. In Sec. II the overall mathematical approach to the phase diagram problem is discussed. It is necessary to go into the method in some detail: only a very careful analysis brings out the nature of the inner phase transition. In Sec. III we will take the free energy and use it to obtain the phase diagram when \mathbf{H} is in the basal plane. The observed tetracritical point comes out in a natural way. By fitting the theory to the longitudinal velocity data we will obtain values for all the relevant parameters of our theory. Then in Sec. IV we will obtain the phase diagram for the case when \mathbf{H} is parallel to the c-axis. We will show that our theory can be fit to the data for the case when \mathbf{H} is parallel to the c-axis with the same set of parameters used for the case when

\mathbf{H} is in the basal plane. The near-crossing of the phase boundaries when \mathbf{H} is along the c -axis is a consequence of approximate particle-hole symmetry. In Sec. V we will discuss the magnetic properties, in particular the magnetic susceptibility. We will show the effect the susceptibility of UPt₃ has on the G-L free energy and how this leads to properties such as the crossing of the upper critical field curves for different directions of the field. In Sec. VI the phase diagram is extended to finite pressure. Finally in Sec. VII we make some concluding remarks.

II. EFFECTIVE FIELD METHOD FOR THE PHASE DIAGRAM

This section will be devoted to explaining the mathematical method used to obtain the phase diagram for UPt₃ in the presence of an external magnetic field. The full problem is very complicated. We give first a simple example to orient the reader to the case of competing order parameters. The reader who is mainly interested in the overall concept, not the details, may read the first subsection and consult the summary figures in the other subsections.

A. Simple model

A simple system with a multicomponent order parameter and competition among the components is a magnet with uniaxial anisotropy. The free energy is:

$$F = \alpha_{0x}(T - T_c)(M_x^2 + M_y^2) + \beta_{xy}(M_x^2 + M_y^2)^2 + \alpha_{0z}(T - T_z)M_z^2 + \beta_z M_z^4 + \beta_{xz}(M_x^2 + M_y^2)M_z^2. \quad (2.1)$$

Suppose that $T_c > T_z$. Then at T_c , the system develops a nonzero M in the x - y plane, its direction otherwise not determined by F . Let us say $\mathbf{M} = M\hat{\mathbf{x}}$ with $M(T)$ given by $\langle M^2 \rangle = \alpha_{x0}(T_c - T)/2\beta_{xy}$. The angle brackets indicate equilibrium values. The question we face (which adumbrates the whole theme of this paper) is: how do M_y and M_z behave below T_c ? The first question has a simple answer. M_y will remain zero below T_c . One way to see this is to write an effective free energy for M_y below T_c by simply taking the terms in F which involve M_y and writing the equilibrium value for M_x and M_z :

$$F_{eff}(M_y) = \alpha_{0x}(T - T_c)M_y^2 + 2\beta_{xy} \langle M_x^2 \rangle M_y^2 + \beta_{xz} \langle M_z^2 \rangle M_y^2 + \beta_{xy}M_y^4 \quad (2.2)$$

$$= \beta_{xz} \langle M_z^2 \rangle M_y^2 + \beta_{xy}M_y^4. \quad (2.3)$$

There will be a temperature range below T_c where $\langle M_z^2 \rangle = 0$. The fact that the effective free energy is then quartic in M_y is the sign that M_x and M_y are degenerate, and the fact that the minimum of F_{eff} is at $M_y^2 = 0$ indicates that rotation of \mathbf{M} in the x - y plane will take place only if a magnetic field (which could be infinitesimal) is applied.

Now do the same for M_z :

$$F_{eff}(M_z) = \alpha_{0z}(T - T_z)M_z^2 + \beta_{xz} \langle M_x^2 \rangle M_z^2 + \beta_z M_z^4 \quad (2.4)$$

$$= [\alpha_{0z}(T - T_z) + \frac{\beta_{xz}}{2\beta_{xy}}\alpha_{0x}(T - T_c)]M_z^2 + \beta_z M_z^4 \quad (2.5)$$

There are evidently two possibilities. Either the expression in square brackets vanishes at positive T , in which case there is a second-order phase transition where M_z appears so that the magnetization rotates in the x - z plane, or it vanishes at negative T , which implies that there is no further transition and $M_z = 0$ at all T . The rotational phase transition, which is second-order, takes place at a lower critical temperature given by

$$T_{c2} = \frac{\alpha_{0z}T_z + (\beta_{xz}\alpha_{0x}/2\beta_{xy})T_c}{\alpha_{0z} + (\beta_{xz}\alpha_{0x}/2\beta_{xy})}. \quad (2.6)$$

An important point is that T_z , the *bare* critical temperature for M_z may be positive but T_{c2} still negative. This would be an example of the effective field suppressing a transition. If there is a transition ($T_{c2} > 0$), then the effective free energy is not valid for $T < T_{c2}$ - it neglects the feedback of M_z on M_x .

Of interest below will be the question of artificial terms such as $\gamma M_x^3 M_z$ in the original free energy. This would add a term $\gamma[\alpha_{0x}(T_c - T)/2\beta_x]^{3/2} M_z$ to the effective free energy for M_z . This means that M_z becomes nonzero already at T_c and the lower transition is converted to a crossover, just as if an external field in the z -direction were applied.

For finding out whether there is a transition, whether it is second order, and computing the lower transition temperature, analysis of the effective free energy is all that is required. To find the behavior of the system below T_{c2} , one must minimize of the full free energy.

B. s-wave superconductor

We now apply the effective field method to the well-known problem of an isotropic s-wave superconductor to show how it works in a case which is actually quite non-trivial, but whose phase diagram is well understood. This system has a single complex order parameter. In the presence of a field, however, there are, in a certain sense, an infinite number of order parameters, and interesting competition among them.

The free energy density for the system is

$$f = \alpha_0(T - T_c) |\eta|^2 + \beta |\eta|^4 + K \sum_i D_i \eta D_i^* \eta^*. \quad (2.7)$$

Here $D_i = -i\partial_i + 2eA_i/\hbar c$ ($-e$ is the charge on an electron) and if we take \mathbf{H} in the z -direction, then the gauge $\mathbf{A} = Hx\hat{\mathbf{y}}$ is appropriate. We have $D_x = -i\partial_x$ and $D_y = -i\partial_y + 2eHx/\hbar c$. Our problem is to minimize the free energy $F = \int f dV$ for arbitrary H and T .

The method we will use is to expand the function $\eta(\mathbf{x})$ in a complete set of normalized eigenfunctions of the operator

$$K(D_x^2 + D_y^2), \quad (2.8)$$

which are

$$\phi_{nk} = [\ell/\pi L_y^2]^{1/4} e^{-iky} \exp[-(x - k\ell^2)^2/2\ell^2] H_n((x - k\ell^2)/\ell), \quad (2.9)$$

where $\ell = \hbar c/2eH$, H_n are the Hermite polynomials, and L_y is the size of the system in the y -direction. We now write

$$\eta(\mathbf{x}) = \sum_{nk} C_{nk} \phi_{nk}(\mathbf{x}) \quad (2.10)$$

and the free energy becomes

$$F = \sum_{nk} [\alpha_0(T - T_c) + \varepsilon_n] |C_{nk}|^2 + \sum_{n_1 k_1, n_2 k_2, n_3 k_3, n_4 k_4} b_{n_1 k_1, n_2 k_2, n_3 k_3, n_4 k_4} C_{n_1 k_1} C_{n_2 k_2}^* C_{n_3 k_3} C_{n_4 k_4}^*. \quad (2.11)$$

The coefficients in this equation are:

$$\varepsilon_n = (n + 1/2) \frac{4KeH}{\hbar c} \quad (2.12)$$

and

$$b_{n_1 k_1, n_2 k_2, n_3 k_3, n_4 k_4} = \beta \int d^3x \phi_{n_1 k_1} \phi_{n_2 k_2}^* \phi_{n_3 k_3} \phi_{n_4 k_4}^*. \quad (2.13)$$

An important point is that ε is independent of k and b is zero unless $k_1 - k_2 + k_3 - k_4 = 0$. We have re-expressed F as a fourth-order polynomial in an infinite number of variables C_{nk} , which may be thought of formally as competing order parameters. We must minimize this polynomial.

The upper critical field curve is given by noticing when the coefficient of the quadratic term *first* changes sign:

$$\alpha_0(T - T_c) + \varepsilon_n = 0; \quad (2.14)$$

The highest value of H for which this equation holds corresponds to $n = 0$ and the curve

$$\alpha_0(T - T_c) + 2KeH/\hbar c = 0 \quad (2.15)$$

defines the normal–superconducting phase boundary.

Below this boundary, some *but not all* of the C_{nk} are nonzero and

$$C_{0k} \sim [\alpha_0(T_c - T) - 2KeH/\hbar c]^{1/2} = \delta^{1/2}. \quad (2.16)$$

This equation defines δ , which serves as a small quantity in the analysis below, the validity of which is thereby limited to the neighborhood of the phase boundary. $\delta > 0$ in the ordered phase. The periodicity of the flux lattice shows that $C_{0k} \neq 0$ if and only if $k = mq$, where m is any integer and $q = \sqrt{\sqrt{3}\pi}/\ell$. We shall denote this condition by $k \in L$, i. e. k belongs to the discrete set which constitutes the flux lattice. The discreteness reflects the fact that magnetic translation symmetry as well as gauge symmetry are broken in the low- T , low- H phase. Thus, sufficiently close to the phase boundary, only these coefficients need be computed and we get the familiar theory of the hexagonal flux lattice. As is well known, no further phase transitions take place as the field is lowered until the Meissner state takes over at H_{c1} .

In UPt_3 , on the other hand, there is another transition when the field is reduced. Why does this not occur in the s-wave case? The answer is not obvious. For example, we may

consider the Landau level $n = 1$. Setting the eigenvalue equal to zero as we did for $n = 0$ would give a critical field line with the same T_c but with a slope only 1/3 of the slope of the H_{c2} curve. Why does no transition take place on this line in the $H - T$ plane? That is, why is there no nonanalytic behavior of the C_{1k} on this line? What about C_{0k} for $k \neq mq$?

To answer these questions, we must develop a picture of the effective fields present in the system when the symmetry has been broken. This is done by classifying different terms of the polynomial in Eq. 2.11.

Class 1: terms determining the leading behavior of C_{0k} , $k \in L$.

These are the simplest of all; the free energy is

$$F = \sum_k [\alpha_0(T - T_c) + \varepsilon_0] |C_{0k}|^2 + \mathcal{O}(C_{0k}^4) + \dots, \quad (2.17)$$

where only the terms relevant to the behavior of terms in class 1 have been written explicitly.

For small δ , these terms give the simple result

$$F = -\delta(C1)^2 + \mathcal{O}((C1)^4) \Rightarrow (C1) \sim \delta^{1/2}, \quad (2.18)$$

where $(C1)$ denote collectively the C_{nk} which belong to class 1. For our considerations which are simply a matter of power counting, the indices on C are not required at this point. The $C1$ are analogous to M_x in the magnetic example. The conclusion is that the C_{nk} are proportional to $\delta^{1/2}$ near the phase boundary.

Class 2: terms determining the leading behavior of $C_{0k'}$, $k' \in L'$.

We write momenta of the form $k' = (m + \frac{1}{2})q$, where m is an integer, with a prime. Combining the $C_{0k'}$ builds a hexagonal lattice which interpenetrates the original one, as we shall see below in section III. When $\delta = 0$ these variables are degenerate with the $(C1)$ - these are the ones not chosen because of the breaking of the magnetic translation symmetry. The $C2$ should be compared to M_y in the previous subsection. As δ increases, they become less favored because they feel an effective repulsion from the $(C1)$. The relevant terms in F (call them collectively $F_{C1,C2}$) are of the form:

$$F_{C1,C2} = \sum_{k'} [\alpha_0(T - T_c) + \varepsilon_0] |C_{0k'}|^2 + \sum_{k_1, k_2, k_3, k_4} b_{0k_1, 0k_2, 0k_3, 0k_4} C_{0k_1} C_{0k_2}^* C_{0k_3} C_{0k_4}^* + \dots \quad (2.19)$$

This equation repays careful examination. A first crucial point is that there are no terms of the form $(C1)^3(C2)$ or $(C1)(C2)^3$. Recall that $b_{n_1 k_1, n_2 k_2, n_3 k_3, n_4 k_4}$ is zero unless $k_1 - k_2 + k_3 - k_4 = 0$. However the $k \in L$ are equally spaced, so if $k_1, k_2, k_3 \in L$, then $k_4 \in L$ as well. Similarly if $k_1, k_2, k_3 \in L'$, then also $k_4 \in L'$. For the case $k_1, k_2 \in L$ then we can have $k_3, k_4 \in L'$. Hence the only cross terms (in L and L') which survive have the form $(C1)^2(C2)^2$. More explicitly,

$$\begin{aligned}
F_{C1,C2} = & \sum_{k'} [\alpha_0(T - T_c) + \varepsilon_0] |C_{0k'}|^2 + \sum_{k_1, k_2, k'_3, k'_4} B_{0k_1, 0k_2, 0k'_3, 0k'_4} C_{0k_1} C_{0k_2}^* C_{0k'_3} C_{0k'_4}^* \quad (2.20) \\
& + \sum_{k_1, k_2, k'_3, k'_4} b_{0k_1, 0k'_3, 0k_2, 0k'_4} C_{0k_1} C_{0k_2} C_{0k'_3}^* C_{0k'_4}^* + c.c. \\
& + \sum_{k'_1, k'_2, k'_3, k'_4} b_{0k'_1, 0k'_2, 0k'_3, 0k'_4} C_{0k'_1} C_{0k'_2}^* C_{0k'_3} C_{0k'_4}^* + \dots
\end{aligned}$$

In this equation

$$B_{0k_1, 0k_2, 0k'_3, 0k'_4} = b_{0k_1, 0k_2, 0k'_3, 0k'_4} + b_{0k_1, 0k_4, 0k'_3, 0k'_2} + b_{0k_3, 0k_4, 0k'_1, 0k'_2} + b_{0k_3, 0k_2, 0k'_1, 0k'_4}. \quad (2.21)$$

In the summations k runs over L and k' runs over L' . The idea of the effective field is to note that, when $H < H_{c2}$ (or $\delta > 0$), we may write an effective free energy for the (C2):

$$\begin{aligned}
F_{eff}((C2)) = & \sum_{k'} [\alpha_0(T - T_c) + \varepsilon_0] |C_{0k'}|^2 \quad (2.22) \\
& + \sum_{k_1, k_2, k'_3, k'_4} B_{0k_1, 0k_2, 0k'_3, 0k'_4} \langle C_{0k_1} C_{0k_2}^* \rangle C_{0k'_3} C_{0k'_4}^* \\
& + \sum_{k_1, k_2, k'_3, k'_4} b_{0k_1, 0k'_3, 0k_2, 0k'_4} \langle C_{0k_1} C_{0k_2} \rangle C_{0k'_3}^* C_{0k'_4}^* + c.c. \\
& + \sum_{k'_1, k'_2, k'_3, k'_4} b_{0k'_1, 0k'_2, 0k'_3, 0k'_4} C_{0k'_1} C_{0k'_2}^* C_{0k'_3} C_{0k'_4}^* + \dots,
\end{aligned}$$

where the angle brackets denote equilibrium values in the ordered phase. Examination of this free energy is all that is required to analyze the stability of L' . Since $C_{0k} \sim \delta^{1/2}$ the structure of this equation is

$$F_{eff}((C2)) = -\delta(1 + R2)(C2)^2 + \mathcal{O}((C2)^4), \quad (2.23)$$

where $R2$ is a dimensionless matrix which is independent of temperature. In fact if the C_{0k} are divided into real and imaginary parts then $R2$ is a real, symmetric matrix. *If there is to be no further phase transition, then all the eigenvalues of $R2$ must be less than or equal to -1.* Otherwise the (C2) condense, and another lattice would form. This would mean an ‘‘inner’’ transition in ordinary s-wave materials, which does not occur. Of course the L' lattice is degenerate with the L lattice. One may be converted into the other with application of an infinitesimal external current as M_x may be converted to M_y in the simple model by an infinitesimal external magnetic field.

Class 3: terms determining the behavior of C_{nk} for $n > 0$ and $k \in L$.

Two subcases must be distinguished here: $n = \text{even}$ and $n = \text{odd}$. If n is even then all possible terms come into the effective free energy for the (C3):

$$\begin{aligned}
F_{eff}((C3)) = & [\alpha_0(T - T_c) + (2n + 1)2KeH/\hbar c](C3)^2 + b3_1 \langle (C1)^3 \rangle (C3) \quad (2.24) \\
& + b3_2 \langle (C1)^2 \rangle (C3)^2 + b3_3 \langle (C1)^3 \rangle (C2)
\end{aligned}$$

where F_{eff} has been written for a definite n value. The coefficient in square brackets is positive as long as $H > H_{c2}/(2n+1)$. b_{31}, b_{32} , and b_{33} are constants independent of δ whose precise form need not detain us. In this field region the leading behavior is dominated by the term linear in the $(C3)$:

$$F_{eff}((C3)) \sim -(C3)^2 + b_{31}(C1)^3(C3) \sim -(C3)^2 + b_{31}\delta^{3/2}(C3) \Rightarrow (C3) \sim \delta^{3/2}. \quad (2.25)$$

This resolves the question raised above. There is no phase transition at $H_{c2}/(2n+1)$ for n even because the coefficients determining the weight of the n th Landau level have already started to grow at H_{c2} itself. Thus the putative phase transition is converted into a crossover.

For $n = \text{odd}$, only even terms in $(C3)$ appear for parity reasons. These remain zero below H_{c2} . One argues in the same way as in case 2; since the $(C3)$ are less stable than the $(C2)$ because of the higher bare quadratic coefficient in front, the conclusion follows *a fortiori*.

Class 4: terms determining the leading behavior of $C_{nk'}$, $n > 0$, $k' \in L'$.

We have accumulated enough experience to write the effective free energy immediately:

$$\begin{aligned} F_{eff}((C4)) = & \sum_{nk'} [\alpha_0(T - T_c) + (2n+1)2KeH/\hbar c] |C_{nk'}|^2 \\ & + 16 \sum_{k_1, k_2, nk'_3, n'k'_4} b_{0k_1, 0k_2, nk'_3, n'k'_4} \langle C_{0k_1} C_{0k_2} \rangle C_{nk'_3} C_{n'k'_4} \\ & + 16 \sum_{k_1, k_2, nk'_3, n'k'_4} b_{0k_1, 0k_2, nk'_3, n'k'_4} \langle C_{0k_1} C_{0k_2} \rangle C_{nk'_3}^* C_{n'k'_4}^* + c.c. \\ & + \sum_{k'_1, k'_2, nk'_3, n'k'_4} b_{0k'_1, 0k'_2, nk'_3, n'k'_4} C_{0k'_1} C_{0k'_2}^* C_{nk'_3} C_{n'k'_4}^* + \dots \end{aligned} \quad (2.26)$$

By analogy with case 2, this may be written as schematically as

$$F_{eff}((C4)) = -\delta(1 + R4)(C4)^2 + \mathcal{O}((C4)^4), \quad (2.27)$$

the only difference being that $R4$ is a matrix in the n index as well as the k' . There are no terms linear in the $(C4)$. There is no phase transition involving the $(C4)$ - hence the eigenvalues of $R4$ are less than -1. The $(C4)$ are always zero in equilibrium.

Class 5: terms determining the behavior of other k values.

It is evident from the momentum conservation condition that the effective free energy for k such that $k \notin L$, $k \notin L'$ can contain terms such as $\langle (C1) \rangle (C5)^3$, for $k = q/3$, for example. There are no terms linear in the $C5$. The cubic terms could give rise to additional first order transitions in principle. It is evident that this does not occur and we do not consider such terms further.

We may conclude this discussion of the s-wave case by a graphical account of how all transitions except the one at H_{c2} itself are suppressed. Fig. 1 shows the bare eigenvalue curves, the repulsion of some levels away from the H_{c2} curve and the conversion to crossover of others. These two effects arise from the effective field coming from the quartic term in the original free energy.

C. Effective field method for the d-wave case

The d-wave case may be analyzed in a similar manner. For our present qualitative discussion we need only the fact that the order parameter becomes a complex two-component vector $\boldsymbol{\eta} = (\eta_x, \eta_y)$. The free energy again contains quadratic and quartic terms in this variable. It is:

$$f = \alpha_0(T - T_x)|\eta_x|^2 + \alpha_0(T - T_y)|\eta_y|^2 + \beta_1(\boldsymbol{\eta} \cdot \boldsymbol{\eta}^*)^2 + \beta_2|\boldsymbol{\eta} \cdot \boldsymbol{\eta}|^2 \quad (2.28)$$

$$+ \sum_{i,j=x,y} (K_1 D_i \eta_j D_i^* \eta_j^* + K_2 D_i \eta_i D_j^* \eta_j^* + K_3 D_i \eta_j D_j^* \eta_i^*) + K_4 \sum_{i=x,y} |D_z \eta_i|^2$$

We have neglected certain terms which are not relevant to the present discussion. They will be introduced in the next section. However, we do not specialize to any particular direction of field, and the analysis is valid for all directions. This section generalizes the analysis carried out by Joynt [21] for the field in the basal plane, which is the easiest case.

The quadratic form may be diagonalized by finding the two-component vector eigenfunctions $\phi_{\mathbf{nk}}$. We then write

$$\boldsymbol{\eta} = \sum_{\mathbf{nk}} C_{\mathbf{nk}} \phi_{\mathbf{nk}} \quad (2.29)$$

to obtain

$$F = \sum_{\mathbf{nk}} [\alpha_0(T - T_{c1}) + \varepsilon_n(H)] |C_{\mathbf{nk}}|^2 \quad (2.30)$$

$$+ \sum_{n_1 k_1, n_2 k_2, n_3 k_3, n_4 k_4} b_{n_1 k_1, n_2 k_2, n_3 k_3, n_4 k_4} C_{n_1 k_1} C_{n_2 k_2}^* C_{n_3 k_3} C_{n_4 k_4}^*$$

the difference with the s-wave case being that the energy levels $\varepsilon_n(H)$ and the form of the b coefficients are far more complicated. Here T_{c1} is the greater of T_x and T_y , and T_{c2}^0 is the lesser of T_x and T_y . The curves which are the lines $\alpha_0(T - T_{c1}) + \varepsilon_n(H) = 0$ are shown in Fig. 2(a). Crucially, however, the momentum conservation condition $k_1 - k_2 + k_3 - k_4 = 0$ is the same. We now specialize a bit to the case of UPt₃. Then the solutions $\alpha_0(T - T_{c1}) + \varepsilon_n(H) = 0$ fall into two classes. Half the levels have a *bare* T_c at T_{c1} [because $\varepsilon_n(H = 0) = 0$] and half at T_{c2}^0 [because $\varepsilon_n(H = 0) = \alpha_0(T_{c1} - T_{c2}^0)$]. Thus when we specify the level index it must be stated to which class the level belongs. Call those with the higher T_c (a) and those with the lower T_c (b). Apart from this difference, the classification of states proceeds similarly to the s-wave case.

1(a): terms determining the leading behavior of $C_{n_a k}$, $n = 0$, $k \in L$.

The free energy is

$$F(C_{0_a k}) = \sum_k [\alpha_0(T - T_{c1}) + \varepsilon_{0_a}] |C_{0_a k}|^2 + \mathcal{O}(C_{0_a k}^4) + \dots, \quad (2.31)$$

with the result that

$$-\delta(C1)_a^2 + \mathcal{O}((C1)_a^4) \rightarrow (C1)_a \sim \delta^{1/2}, \quad (2.32)$$

where $\delta = -[\alpha_0(T - T_{c1}) + \varepsilon_{0_a}]$.

Class 2(a): terms determining the leading behavior of $C_{0_a k'}$, $k' \in L'$.

Again, we write momenta of the form $(m + \frac{1}{2})q$, where m is an integer, with a prime. These coefficients may be treated by analogy with the s-wave class 2 above. Familiar with the procedure, we may write down the relevant effective free energy immediately:

$$F_{eff}((C2)_a) = -\delta(1 + R2_a)(C2)_a^2 + \mathcal{O}((C2)_a^4), \quad (2.33)$$

where again $R2_a$ is a dimensionless matrix. This matrix is similar to $R2$, and we expect that all the eigenvalues of $R2_a$ must be less than or equal to -1 and the usual hexagonal symmetry arises at H_{c2} . That this is actually the case has been shown by Luk'yanchuk and Zhitomirskii. [22].

Class 3(a): terms determining the behavior of $C_{n_a k}$ for $n > 0$ and $k \in L$.

The analysis proceeds as in s-wave class 3.

$$F_{eff}((C3)_a) \sim (C3)_a^2 + b3_{1a}(C1)_a^3(C3)_a \sim (C3)_a^2 + b3_{1a}\delta^{3/2}(C3)_a \rightarrow (C3)_a \sim \delta^{3/2}. \quad (2.34)$$

These candidate phase transitions are thus converted to crossovers by the effective field. Note that there is, for general field directions, no parity selection rule in the d-wave case so there is no distinction between $n = \text{odd}$ and $n = \text{even}$. The $(C3)_a$ contribute to the change of shape of the vortices as the external field is reduced below H_{c2} , but produce no further phase transition.

Class 4(a): terms determining the leading behavior of $C_{n_a k'}$, $n_a > 0$, $k' \in L'$.

The effective free energy is:

$$F_{eff}((C4)_a) = -\delta(1 + R4_a)(C4)_a^2 + \mathcal{O}((C4)_a^4). \quad (2.35)$$

We again argue by analogy with s-wave case 4 that the eigenvalues of $R4_a$ must be less than -1 so that the $(C4)_a$ are always zero.

Class 5(a): other periodicities.

Again other periodicities will not arise from states in class a, just as in s-wave, case 5.

In discussing cases 1(a) to 5(a), we stress that we have not given explicit proofs for the magnitude of the eigenvalues of the different R -matrices. It is possible to write these matrices formally, but they are quite complicated. However, they are very similar to the s-wave case, where we are certain of the result even in the absence of explicit calculation.

Let us now turn to the the levels which start from T_{c2}^0 . Here we have less guidance from the s-wave analogy.

Class 1(b): terms determining the leading behavior of $C_{0_b k}$, $k \in L$.

These terms are analogous to those in s-wave class 3. As long as $H \neq 0$, all possible terms come into the effective free energy for the $(C1)_b$:

$$F_{eff}((C1)_b) = [\alpha_0(T - T_{c1}) + \varepsilon_{0_b}](C1)_b^2 + b3_{1ab} \langle (C1)_a^3 \rangle (C1)_b \quad (2.36)$$

$$+ b3_{2ab} \langle (C1)_a^2 \rangle (C1)_b^2 + b3_{3ab} \langle (C1)_a^3 \rangle (C1)_b.$$

For certain special directions of the field, the cubic-linear and linear-cubic terms may vanish, but we are concerned here with the general case. This leads to the result that

$$F_{eff}((C1)_b) \sim (C1)_b^2 + b3_{1ab}(C1)_a^3(C2)_b \sim (C1)_b^2 + b3_{1ab}\delta^{3/2}(C1)_b \rightarrow (C1)_b \sim \delta^{3/2}. \quad (2.37)$$

Thus these terms show crossover behavior. This fact is the apparent basis for a statement occasionally found in the literature that for general directions of the field there is no lower phase transition in d-wave systems at finite field [23,18].

Class 2(b): terms determining the leading behavior of $C_{0_{k'}}$, $k' \in L'$.

This is the crucial case so we treat it in detail. The relevant terms in F_{eff} are:

$$F_{eff}((C2)_b) = \sum_{k'} [\alpha_0(T - T_{c1}) + \varepsilon_{0_b}] |C_{0_b k'}|^2 \quad (2.38)$$

$$+ \sum_{k_1, k_2, k'_3, k'_4} B_{0_a k_1, 0_a k_2, 0_b k'_3, 0_b k'_4} \langle C_{0_a k_1} C_{0_a k_2}^* \rangle C_{0_b k'_3} C_{0_b k'_4}^*$$

$$+ \sum_{k_1, k_2, k'_3, k'_4} b_{0_a k_1, 0_b k'_3, 0_a k_2, 0_b k'_4} \langle C_{0_a k_1} C_{0_a k_2} \rangle C_{0_b k'_3}^* C_{0_b k'_4}^* + c.c.$$

$$+ \sum_{k'_1, k'_2, k'_3, k'_4} b_{0_a k'_1, 0_a k'_2, 0_b k'_3, 0_b k'_4} \langle C_{0_a k'_1} C_{0_a k'_2}^* \rangle C_{0_b k'_3} C_{0_b k'_4}^* + \dots,$$

where the angle brackets denote equilibrium values in the ordered phase and

$$B_{0_a k_1, 0_a k_2, 0_b k'_3, 0_b k'_4} = b_{0_a k_1, 0_a k_2, 0_b k'_3, 0_b k'_4} + b_{0_a k_1, 0_b k_4, 0_b k'_3, 0_a k'_2} \quad (2.39)$$

$$+ b_{0_b k_3, 0_b k_4, 0_a k'_1, 0_a k'_2} + b_{0_b k_3, 0_a k_2, 0_a k'_1, 0_b k'_4}$$

Since $C_{0_{ak}} \sim \delta^{1/2}$ the structure of this equation is

$$F_{eff}((C2)_b) = [\alpha_0(T - T_{c1}) + \varepsilon_{0_b} - \delta R2_b](C2)_b^2 + \mathcal{O}((C2)_b^4), \quad (2.40)$$

where again $R2_b$ is a dimensionless matrix. The question of further phase transitions in this case boils down to asking whether the matrix $[\alpha_0(T - T_{c1}) + \varepsilon_{0_b} - \delta R2_b]$ can ever have negative eigenvalues. If it does, then there will be a lower phase transition. The answer is known for UPt_3 (more formally for E representations of the hexagonal group in some parameter ranges) in certain limiting cases. If $H = 0$, then the problem reduces to a well-known one [24,9,10]. There are indeed two transitions and the effect of $\delta R2_b$ is to reduce the bare transition temperature T_{c2}^0 (where $\alpha_0(T - T_{c1}) + \varepsilon_{0_b}(H = 0) = 0$) to T_{c2} , the observed

lower transition temperature. This is the precise analog of the critical temperature for M_z in Eq. 2.6. Also for \mathbf{H} in the basal plane and arbitrary field strength, the problem can be solved [21]. At the tetracritical point, $\delta R2_b$ vanishes, so there is no effective field. Near this point, the effective fields can be calculated, and we will carry this calculation out in the next section. $[\alpha_0(T - T_{c1}) + \varepsilon_{0_b} - \delta R2_b]$ vanishes along a line in H - T space. This represents the second phase transition for this field direction. In fact all the functions involved are continuous and the second phase transition occurs for all directions of \mathbf{H} for UPt_3 .

Class 3(b): terms determining the behavior of $C_{n_b k}$ for $n_b > 0$ and $k \in L$.

The interesting new feature that arises for these terms is that we now have an effective field from both the $(C1)_a$ and the $(C2)_b$. There are more terms in the effective free energy for the $(C3)_b$. However, we shall not consider this in detail, since it is evident that these $(C3)_b$ couple linearly to the $(C1)_a$ and therefore start their life at $H_{c2}(T)$ where they are proportional to $\delta^{3/2}$.

Class 4(b): terms determining the leading behavior of $C_{n k'}$, $n > 0$, $k' \in L'$.

Here the relationship of terms $(C4)_b$ to $(C2)_b$ is the same as that s-wave $(C3)$ to s-wave $(C1)$. Thus there is an effective free energy of the form:

$$F_{\text{eff}}((C4)_b) \sim [\alpha_0(T - T_{c1}) + \varepsilon_{n_b}](C4)_b^2 + \mathcal{O}((C2)_b^3(C4)_b). \quad (2.41)$$

Crossovers only are allowed for these terms.

Class 5(b): other periodicities.

We may neglect these for the same reasons as s-wave class 5.

Let us now summarize the conclusions. At H_{c2} the $C_{0_a k}$ condense to form a hexagonal lattice which we call L . At the same time, a number of other coefficients begin to grow (such as those in class 3(a) and 1(b)), though more slowly than the $C_{0_a k}$. Their growth means that the shape of the vortices is temperature and field-dependent, but the symmetry of the lattice L is unchanged. As the temperature or field is further lowered, the $C_{0_b k'}$ become unstable, forming a lattice L' which interpenetrates L . This occurs by a second-order phase transition. This process is summarized in Fig. 2.

III. PHASE DIAGRAM: FIELD IN THE BASAL PLANE

We have now established the mathematical method for finding the phase boundaries. In this section we apply the method to the *quantitative* construction of the phase diagram for the case when the field is in the basal plane of the hexagonal UPt_3 crystal. We begin by writing down the free energy density for a hexagonal E_1 or E_2 system:

$$\begin{aligned}
f = & \alpha_0(T - T_x)|\eta_x|^2 + \alpha_0(T - T_y)|\eta_y|^2 + \beta_1(\boldsymbol{\eta} \cdot \boldsymbol{\eta}^*)^2 + \beta_2|\boldsymbol{\eta} \cdot \boldsymbol{\eta}|^2 \\
& + \sum_{i,j=x,y} (K_1 D_i \eta_j D_i^* \eta_j^* + K_2 D_i \eta_i D_j^* \eta_j^* + K_3 D_i \eta_j D_j^* \eta_i^*) + K_4 \sum_{i=x,y} |D_z \eta_i|^2 \\
& + (\alpha_0 \epsilon \Delta T) (\hbar c / 2e) \sum_{i=x,y} (|D_i \eta_x|^2 - |D_i \eta_y|^2) \\
& + a_z H_z^2 \boldsymbol{\eta} \cdot \boldsymbol{\eta}^* + a_x (H_x^2 + H_y^2) \boldsymbol{\eta} \cdot \boldsymbol{\eta}^* + a_d |\mathbf{H} \cdot \boldsymbol{\eta}|^2.
\end{aligned} \tag{3.1}$$

Here $\boldsymbol{\eta} = (\eta_x, \eta_y)$ is the two-component order parameter, and $K_1, K_2, K_3, K_4, \alpha_0, \beta_1, \beta_2, a_x, a_z, a_d$ and ϵ are constants. The coupling of the staggered magnetization to $\boldsymbol{\eta}$ is responsible for the temperature splitting $\Delta T = T_x - T_y$. The terms quadratic in H are Pauli limiting terms. They arise due to the reduction of the spin susceptibility in the singlet superconducting state. The effect of these terms on the phase diagram and a physical explanation for the relative sizes which we obtain for the various a coefficients will be given in Sec. V. The phase diagram for the case of the field in the basal plane in our theory has been considered previously by Joynt [21], but we now wish to consider it in more detail and compare our results to experimental data. Similar calculations have also been performed in other models. [25,26]

It has been suggested that the spatial variation of $\boldsymbol{\eta}$ along the field direction needs to be considered in the calculation of the upper critical field. [18] To show that this does not occur, we have computed the eigenvalues for the quadratic part of Eq. 3.1 as a function of p^2 , the wavevector along the field direction. The coefficient of p^2 is positive, meaning that $\boldsymbol{\eta}$ is uniform along the direction of the field, unless $(K_2 + K_3)/K_1 > 3.126$. As we shall see below, this is certainly larger than any value which can fit the upper critical field data. In fact the ratio is roughly unity. Let us choose a coordinate system such that $\mathbf{H} = H \hat{\mathbf{x}}$. In this system, the result is that we can minimize any terms in the free energy density containing D_x by setting them to zero. Our free energy density is then

$$\begin{aligned}
f = & \alpha_0(T - T_y)|\eta_y|^2 + (\beta_1 + \beta_2)|\eta_y|^4 + K_4|D_z \eta_y|^2 + K'_{123}|D_y \eta_y|^2 \\
& + \alpha_0(T - T_x)|\eta_x|^2 + (\beta_1 + \beta_2)|\eta_x|^4 + K_4|D_z \eta_x|^2 + K'_1|D_y \eta_x|^2 \\
& + 2\beta_1|\eta_x|^2|\eta_y|^2 + \beta_2(\eta_x^{*2}\eta_y^2 + \text{C.C.})
\end{aligned} \tag{3.3}$$

In this equation $K_{123} = K_1 + K_2 + K_3$, $K'_{123} = K_{123} - (\alpha_0 \epsilon \Delta T)(\hbar c / 2e)$, and $K'_1 = K_1 + (\alpha_0 \epsilon \Delta T)(\hbar c / 2e)$.

The upper critical fields of the separate components η_x (H_{c2x}) and η_y (H_{c2y}) are now easy to calculate, though the equations for the phase boundary are more conveniently expressed in terms of the inverse functions $T_{c2x}(H)$ and $T_{c2y}(H)$. We obtain

$$T_{c2x} = -((a_x + a_d)/\alpha_0)H^2 + H/S_{c2x} + T_x \tag{3.4}$$

$$T_{c2y} = -(a_x/\alpha_0)H^2 + H/S_{c2y} + T_y \tag{3.5}$$

where $S_{c2x} = -(\hbar c / 2e)(\alpha_0 / \sqrt{K_4 K'_1})$ and $S_{c2y} = -(\hbar c / 2e)(\alpha_0 / \sqrt{K_4 K'_{123}})$. S_{c2x} and S_{c2y} are the slopes of the respective H_{c2} curves at zero field. For a_x and a_d small (as we assume) and if $T_y > T_x$ and $K'_{123} > K'_1$ then the two upper critical field curves cross. The physical phase boundary is the greater of the two and we obtain the well-known kink in H_{c2} for this direction of the field. We now want to find expressions for the two inner transition lines $H_y^*(T)$ and $H_x^*(T)$.

Consider a fixed temperature T such that $H_{c_{2y}}(T) > H_{c_{2x}}(T)$ and ask what happens as the field is reduced starting from a field $H > H_{c_{2y}}(T)$. As the field is lowered below $H_{c_{2y}}(T)$ we will have $\eta_x = 0$ but $\eta_y \neq 0$. From the parts of the free energy involving only η_y we immediately see that η_y will form a lattice. However, the lattice will be distorted from pure hexagonal because $K_4 \neq K'_{123}$ in general. If we choose the gauge $\mathbf{A} = -Hz\hat{\mathbf{y}}$ we obtain

$$\eta_y = N_y \sum_n c_n \exp(inqy - (z - nq\ell^2)^2 / (2r_y^2\ell^2)). \quad (3.6)$$

In this equation $r_y^2 = \sqrt{K_4/K'_{123}}$, N_y is the (real) magnitude of η_y , and $q = \sqrt{\sqrt{3}\pi}(r_y/\ell)$. Finally, $c_n = 1$ if n is even and $c_n = i$ if n is odd. The lattice formed by $|\eta_y|$ is a centered rectangular lattice, although it is perhaps more clearly imagined as a triangular lattice which has been “stretched” by the anisotropy. The side of the unit cell parallel to $\hat{\mathbf{y}}$ has a length of $2\pi/q$, while the side parallel to $\hat{\mathbf{z}}$ has a length $q\ell^2$.

Suppose now that we are at a temperature T such that $H_{c_{2x}}(T) > H_{c_{2y}}(T)$ and we lower the field starting from $H > H_{c_{2x}}(T)$. In this case as the field is lowered we will first come to a region where $\eta_x \neq 0$ and $\eta_y = 0$. We may then find η_x in precisely the same way as we found η_y above. Using the same gauge as before we have

$$\eta_x = N_x \sum_n c_n \exp(inqy - (z - nq\ell^2)^2 / (2r_x^2\ell^2)). \quad (3.7)$$

Here, however, we have $r_x^2 = \sqrt{K_4/K'_1}$ and $q = \sqrt{\sqrt{3}\pi}(r_x/\ell)$.

Let us return to the first case where we lower the field at constant T and $H_{c_{2y}}(T) > H_{c_{2x}}(T)$ and ask what happens as the field is lowered below $H_{c_{2y}}(T)$. Eventually the field will be low enough so that the free energy is minimized with both $\eta_x \neq 0$ and $\eta_y \neq 0$. The point where this occurs is $H_x^*(T)$. To calculate $H_x^*(T)$ formally we need to follow the prescription of Sec. II: substitute in the functional forms for η_x and η_y into f , compute the free energy $F = \int f dV$, and determine when the coefficient of the term quadratic in N_x changes sign.

We must choose the functional form of η_x very carefully in this calculation for three reasons. First, we must allow the singularities of the η_x flux lattice to be located at different points than the singularities of the η_y flux lattice while still insuring that η_x has a form appropriate to the gauge we have chosen. Second, we need to allow η_x and η_y to have different phases. Finally, since η_x is arising in the effective periodic potential formed by η_y , we know that η_x will have the same periodicities as η_y . (This is an application of Bloch’s theorem [21]). Hence we write

$$\eta_x = N_x e^{i\theta} \sum_n c_n \exp(i(nq + z_0/\ell^2)(y - y_0) - (z - z_0 - nq\ell^2)^2 / (2r_x^2\ell^2)) \quad (3.8)$$

with $q = \sqrt{\sqrt{3}\pi}(r_y/\ell)$.

After minimizing the free energy with respect to the phase difference θ the free energy is

$$F = \alpha_0 [T - T_{c_{2y}}(H)] \langle |\eta_y|^2 \rangle + (\beta_1 + \beta_2) \langle |\eta_y|^4 \rangle \quad (3.9)$$

$$\begin{aligned} & + \alpha_0 [T - T_{c_{2x}}(H)] \langle |\eta_x|^2 \rangle + (\beta_1 + \beta_2) \langle |\eta_x|^4 \rangle \\ & + 2\beta_1 \langle |\eta_x|^2 |\eta_y|^2 \rangle - 2\beta_2 \langle \eta_x^{*2} \eta_y^2 e^{2i\theta} \rangle \\ & = \langle f_x \rangle + \langle f_y \rangle + 2\beta_1 I_1 - 2\beta_2 |I_2|. \end{aligned} \quad (3.10)$$

Here the angle brackets denote a spatial average ($\langle \dots \rangle = \int \dots dV$), f_x (f_y) is the part of the free energy density that depends only on η_x (η_y), $I_1 \equiv \langle |\eta_x|^2 |\eta_y|^2 \rangle$, and $I_2 \equiv \langle \eta_x^{*2} \eta_y^2 e^{2i\theta} \rangle$. The inner transition ($H_x^*(T)$) occurs when the term quadratic in η_x changes sign or when

$$\alpha_0 [T - T_{c2x}(H_x^*)] \langle |\eta_x|^2 \rangle + 2\beta_1 I_1 - 2\beta_2 |I_2| = 0. \quad (3.11)$$

This equation contains N_y^2 which is determined by minimizing $\langle f_y \rangle$ which gives us

$$\alpha_0 [T - T_{c2y}(H_x^*)] \langle |\eta_y|^2 \rangle + 2(\beta_1 + \beta_2) \langle |\eta_y|^4 \rangle = 0. \quad (3.12)$$

We may now solve for $H_x^*(T)$. Once again, however, it is easier to express the result in terms of the inverse function $T_x^*(H)$. We obtain

$$T_x^*(H) = -(a_x^*/\alpha_0)H^2 + H/S_x^* + T_{x_0}^* \quad (3.13)$$

where

$$a_x^* = \frac{(a_x + a_d) - Q_y a_x}{1 - Q_y}, \quad (3.14)$$

$$S_x^* = \frac{S_{c2x} S_{c2y} (1 - Q_y)}{S_{c2y} - Q_y S_{c2x}}, \quad (3.15)$$

$$T_{x_0}^* = \frac{T_x - Q_y T_y}{1 - Q_y}. \quad (3.16)$$

Here

$$Q_y \equiv \frac{\beta_1 I_1 - \beta_2 |I_2|}{(\beta_1 + \beta_2) \beta_A \langle |\eta_x|^2 \rangle \langle |\eta_y|^2 \rangle} \quad (3.17)$$

where β_A is the Abrikosov lattice parameter: $\beta_A = \langle |\eta_y|^4 \rangle / (\langle |\eta_y|^2 \rangle)^2$. Note that we may rewrite our result as

$$T_x^*(H) = T_{c2x}(H) - \left(\frac{Q_y}{1 - Q_y} \right) [T_{c2y}(H) - T_{c2x}(H)]. \quad (3.18)$$

From this equation we see that the the inner transition line for η_x is repelled away from the calculated upper critical field curve for η_x by an amount proportional to the separation between the calculated upper critical field curves for η_y and η_x .

For the opposite case, when we consider lowering the field starting from a temperature T such that $H_{c2x}(T) > H_{c2y}(T)$, the calculation proceeds precisely as before. The inner transition line, T_y^* , for this case is related to the calculated outer transition lines as in Eq. 3.18 so that

$$T_y^*(H) = T_{c2y}(H) - \left(\frac{Q_x}{1 - Q_x} \right) [T_{c2x}(H) - T_{c2y}(H)]. \quad (3.19)$$

Here Q_x is given by Eq. 3.17. However, since η_y is becoming non-zero in the periodic potential formed by η_x the periodicity of the flux lattices is set by η_x . This means that for this calculation $q = \sqrt{\sqrt{3}\pi}(r_x/\ell)$.

We now must calculate the integrals I_1 and I_2 . This is a straightforward but tedious exercise and we omit the details. We only note here that the results do not depend on r_x and r_y separately but only on the ratio r_x/r_y . This is significant for curve-fitting because although r_x and r_y cannot be obtained from the phase diagram when \mathbf{H} is in the basal plane their ratio can be obtained through $(r_x/r_y)^2 = S_{c2x}/S_{c2y}$. This equation follows directly from the definitions of the quantities involved.

We also note that while I_1 is non-zero for all values of the offset vector $\mathbf{v} = y_0\hat{\mathbf{y}} + z_0\hat{\mathbf{z}}$, I_2 is zero unless \mathbf{v} is a flux lattice vector or one-half of a flux lattice vector [26]. In other words if $\mathbf{u}_1 = (2\pi/q)\hat{\mathbf{y}}$ and $\mathbf{u}_2 = (\pi/q)\hat{\mathbf{y}} + q\ell^2\hat{\mathbf{z}}$ are the basis vectors of the flux lattice then I_2 is zero unless $\mathbf{v} = \frac{1}{2}(n\mathbf{u}_1 + m\mathbf{u}_2)$, where n and m are integers. By symmetry there are only three distinct offset points in the Wigner-Seitz primitive unit cell of the flux lattice where I_2 is non-zero. These are the d ($\mathbf{v} = 0$), c ($\mathbf{v} = \frac{1}{2}\mathbf{u}_1$), and b ($\mathbf{v} = \frac{1}{2}\mathbf{u}_2$) points, as shown in Fig. 3. Consequently, by the definition of the Q 's (Eq. 3.17), Q_x and Q_y will have their smallest values when \mathbf{v} is at one of these points. By the equations for the inner transition lines (Eqs. 3.18 and 3.19) when Q is at its smallest the inner transition line is closest to the outer transition line. Hence, the inner transition line which is actually observed is the transition line which corresponds to the smallest value of Q . Hence, we see that the inner transition line must correspond to an offset vector which is at one of points d, c, or b.

To determine which offset vector is favored and to fit our theory to the experimentally observed phase diagram we must calculate Q_y , and from it $T_x^*(H)$, and Q_x , and from it $T_y^*(H)$. Along with the parameters that can be obtained by requiring that the outer transition lines fit the data (T_x , S_{c2x} , a_d , T_y , S_{c2y} , a_x) we also need β_2/β_1 in order to perform the calculation. This ratio may be determined in from the specific heat jumps at zero field at the outer ($\Delta C_V(T_y)$) and inner ($\Delta C_V(T_{x_0})$) transitions using

$$\frac{\beta_2}{\beta_1} = \frac{\Delta C_V(T_{x_0})/T_{x_0}}{\Delta C_V(T_y)/T_y} - 1. \quad (3.20)$$

From data for the specific heat jumps [27] we obtain $\beta_2/\beta_1 = 0.5$.

The phase diagram we obtain from our calculations is shown along with the ultrasonic velocity data from Ref. [5] in Fig. 4 along with the values of the parameters used to obtain it. We find that for our fit to the phase diagram the offset vector is at the b point. The fit is very good for the outer transition lines and $H_x^*(T)$ but poor for $H_y^*(T)$. The problems fitting $H_y^*(T)$ are not difficult to understand. The inner transition lines are given by equations such as Eq. 3.19. These equations state that the inner transition lines are repelled from the continuation of the corresponding outer transition line by an amount which is proportional (in the case of Eq. 3.19) to $Q_x/(1-Q_x)$. The quantity Q_x has been calculated in the limit of very small δ , i. e. near the tetracritical point. Unlike the other quantities calculated, however, Q_x is expected to have very strong nonlinearities. The first term in Q_x is proportional to

$$\frac{\langle |\eta_x|^2 |\eta_y|^2 \rangle}{\langle |\eta_x|^2 \rangle \langle |\eta_y|^2 \rangle}. \quad (3.21)$$

This quantity is considerably less than one when the separation of the vortices is comparable to the core size at the tetracritical point. We find $Q_x = 0.333$ (see below). When $H < H_{c2}$,

however, the core size quickly becomes smaller than the separation and $|\eta_x|^2$ and $|\eta_y|^2$ are constant except in the region of the cores, only a small fraction of the volume. Inspection of Eq. 3.21 shows that $Q_x \rightarrow 1$ and $Q_x/(1 - Q_x)$ becomes large. This magnifies the repulsion between $H_{c2y}(T)$ and $H_y^*(T)$ and therefore the repulsion between the phase boundaries $H_{c2x}(T)$ and $H_y^*(T)$.

This brings in an additional error: the breakdown of the our approximation for the form of the order parameter. We assumed that both η_x and η_y were formed by the usual linear combination of lowest Landau levels. This assumption is strictly correct only at the tetracritical point where the inner and outer transition lines meet. It remains a reasonable assumption as long as the inner transition line is not repelled too far away from the outer transition line. These problems are not so serious for $H_x^*(T)$, because in this case the curve fits smoothly to the zero-field point, which is exact. There is no such additional constraint for $H_y^*(T)$. It is therefore necessary to incorporate some nonlinear effects in the fit to this line. The slope at the tetracritical point itself is correctly given by the linear calculation. Over the length of the line, however, we use a renormalized \tilde{Q}_x given by fitting the slope. Both renormalized and unrenormalized fits are given in Fig. 4.

IV. PHASE DIAGRAM: FIELD ALONG THE C-AXIS

In this section we wish to take the free energy, Eq. 3.1, and use it to compute the phase diagram when the field is along the c-axis (the z -direction) of the crystal. The procedure for finding the outer transition line (the upper critical field curve) in our theory for arbitrary angles of the field with the c-axis has been developed elsewhere. [28,22] We briefly review the procedure.

To find the upper critical field at an arbitrary field direction one first follows the Euler-Lagrange prescription and demands that variations in the free energy F with respect to each component of the order parameter vanish. This condition gives two G-L equations which for purposes of finding H_{c2} may be linearized. The linearized G-L equations may be viewed as a Schrödinger equation for $\boldsymbol{\eta}$. This defines an effective hamiltonian which is a 2×2 matrix in the components of $\boldsymbol{\eta}$. One then defines a new coordinate system with one axis along the field and the other two axes perpendicular to it.

It is easy to show that the component of the \mathbf{D} operator along the field (D_1) commutes with the components in the other two directions. Hence D_1 commutes with the effective hamiltonian and we may rewrite any terms containing $D_1\boldsymbol{\eta}$ as $p_1\boldsymbol{\eta}$ where p_1 is a c-number. When the field is in the z -direction the only terms which result from this substitution are terms proportional to p_1^2 , which are minimized by setting $p_1 = 0$. Therefore in this case, as in the less obvious case when the field is in the basal plane, one may simplify the G-L equations by setting $D_1\boldsymbol{\eta} = 0$. Since this procedure may be done both when the field is in the z -direction and in the seemingly least favorable case when the field is in the basal plane it is reasonable to assume that it may be done for any angle the field makes with the z -axis.

One then defines raising and lowering operators $D_{\pm} = \ell(rD_2 \pm iD_3/r)/\sqrt{2}$ and $\eta_{\pm} = (\eta_x \pm i\eta_y)/2$. Here r is a function of the angle the field makes with the c-axis and is chosen to simplify the G-L equations as much as possible. One can then rewrite the G-L equations in terms of these quantities and expand η_+ and η_- in terms of the states $|n\rangle$:

$$\eta_+ = \sum_n a_n |n\rangle \quad \eta_- = \sum_n b_n |n\rangle. \quad (4.1)$$

Here $D_+D_- |n\rangle = n |n\rangle$. The states $|n\rangle$ are quasi-Landau levels. The problem then splits into finding the eigenvalues of an infinite tri-diagonal matrix. From the lowest eigenvalue one can then compute H_{c2} .

Finding the inner transition line near to the upper critical field is also a linear problem, as the analysis of Sec. II demonstrated. To find the line rigorously we would have to calculate the effective free energy for all of the eigenfunctions due to the presence of the eigenfunction with the lowest eigenvalue, as outlined in Sec. II. However, we have seen that the only transition line which is not destroyed (that is, either converted to a crossover or repelled to non-physical fields and temperatures) by the coupling to the lowest eigenfunction is the line which originates at the inner transition temperature and corresponds to a flux lattice shifted from the flux lattice formed by the lowest eigenfunction. The full effective field matrix therefore contains levels which are pushed to unphysical fields (pushed up to high energy in the quantum-mechanical analogy), or have small magnitude ($\sim \delta^{3/2}$). Thus, rather remarkably, it will be a very good approximation to compute the inner transition line using only two levels. As in the case when the field is in the basal plane we then have a correction to the bare inner transition line which is proportional to the separation between the bare inner transition and the outer transition in order to find the actual inner transition line. Our formula for the inner transition line $T_{inner}(H)$ in terms of the bare inner transition line $T_{bare}(H)$ and the outer transition line $T_{outer}(H)$ is then

$$T_{inner}(H) = T_{bare}(H) - g[T_{outer}(H) - T_{bare}(H)]. \quad (4.2)$$

When the field was in the basal plane we were able to compute the coupling constant g . For the field along the c -axis this computation, though straightforward in principle, is exceedingly complicated. Accordingly, g is found by fitting to the data.

A key feature of the bare inner transition line comes to light upon examining the matrix used to find it. This matrix is

$$\begin{pmatrix} (2K_1 + K) - K' & -\alpha_0 \ell^2 \Delta T (2\epsilon H - 1) \\ -\alpha_0 \ell^2 \Delta T (2\epsilon H - 1) & (2K_1 + K) + K' \end{pmatrix}. \quad (4.3)$$

Here $K = K_2 + K_3$ and $K' = K_2 - K_3$. Note that the off-diagonal terms will vanish when $H = 1/2\epsilon$. This means that if $K' \approx 0$, as is expected from particle-hole symmetry [29], the two eigenvalues will be nearly degenerate at this H and the outer and bare inner transition lines will nearly touch. This cancellation between the derivative terms in the free energy (Eq. 3.1) proportional to K_2 and K_3 and the terms which couple the staggered magnetization (through ΔT) to the derivatives means we obtain an *apparent* tetracritical point - the two lines come close but do not quite touch. There are *only two* superconducting phases when the field is in the z -direction or indeed for any direction except in the basal plane. The fact that K' depends sensitively on the impurity density has interesting consequences. The minimum separation will depend on this density. Unfortunately, the sharpness of these transitions also depends on the impurity density.

The phase diagram we obtain from our calculations with the field in the z -direction together with the values of the parameters used to obtain it and the ultrasonic velocity data

from Ref. [5] is shown in Fig. 5. Note that we use the same parameters as for our fit for when the field is in the basal plane along with some additional parameters. As was the case when the field was in the basal plane the fit is very good except for the high-field, low-temperature part of the inner phase boundary where the linear theory is expected to break down. This happens because of the renormalizations discussed in the previous section.

A virtue of the theory given here is that a striking difference between the phase diagrams for the two directions of the field receives an explanation. The upper critical field curve is smoother for field along the c -axis, and the inner transition line is much smoother. This can now be seen to result from the ‘hybridization’ of the two curves for this case, the presence of the off-diagonal matrix elements in Eq. 4.3. This is absent for the other field direction, when the two components decouple.

V. MAGNETIC PROPERTIES OF UPt_3

In this section we wish to discuss the origin, effect, and relative sizes of the Pauli limiting terms in the free energy density. These are the terms proportional to $H^2\eta^2$ in Eq. 3.1. In order to do this, we require some preliminary background about magnetic properties of the normal state. The first fact to appreciate is that the magnetic susceptibility χ_{ij} of the normal state is enhanced by roughly the same factor as the mass. Because χ_{ij} is large, the Pauli limiting effect of the field on superconductivity is likely to be appreciable. The second important point is that the susceptibility is anisotropic, and the temperature dependences of the components are different. This is clear from the plots of the susceptibilities $\chi_{xx}(T)$ and $\chi_{zz}(T)$ in Fig. 6. $\chi_{xx}(T) > \chi_{zz}(T)$ at all temperatures. [30] At high T , both functions take on the local moment form $\chi \sim 1/T$, while each goes to a finite constant, characteristic of Pauli or van Vleck behavior, at low T . In addition, $\chi_{xx}(T)$ has an anomaly around 15 K.

Let us first take a theoretical approach to understanding the anisotropy in χ_{ij} . Our basic assumption is that UPt_3 is a Fermi liquid at temperatures just above the critical temperature. Then the starting point is the single-particle states calculated in band theory, which account very well for the Fermi surface. [32] The states near the Fermi surface are predominantly derived from uranium 5f orbitals with $j = 5/2$, as would be expected from Hund’s rules for an actinide system with a 5f occupancy near 2. In the isolated atom, the $j = 5/2$ level is 6-fold degenerate. In the hexagonal crystal field, there is an effective Hamiltonian at the Γ point which splits the six-fold degenerate state into three doublets at the Γ point: $j_z = \pm 5/2$, $j_z = \pm 3/2$, and $j_z = \pm 1/2$. This means that UPt_3 is likely to be an example of a system in which the magnetism is Van Vleck-like in the plane and Pauli-like along the c -axis, which is expected to be a general feature of hexagonal U-based systems. [33].

Let us briefly review the reasons for this expectation. If we apply a magnetic field, there will be both a Pauli (inraband) and a Van Vleck (interband) contribution to the susceptibility. The former is of order $(g_{\text{eff}}\mu_B)^2 N(\varepsilon_F)$, while the latter is of order $(g_{\text{eff}}\mu_B)^2/|B_h|$. Here g_{eff} is an effective g-factor for the coupling of the field to the total angular momentum of the band or bands involved. It is a dimensionless number of order unity. The Landé factor for $\ell=3$, $s=1/2$, and $j=5/2$ is 6/7. B_h is the separation between the bands and $N(\varepsilon_F)$ is the density of states at the Fermi energy. The Van Vleck susceptibility is given by

$$\chi_{ii} = 2n\mu_B^2 \sum_{\alpha,\beta} \frac{|\langle \alpha | L_i + 2S_i | \beta \rangle|^2}{E_\beta - E_\alpha} f_\alpha (1 - f_\beta). \quad (5.1)$$

Here f_α , f_β , E_α , E_β are occupation factors and energies of the states α and β . In view of the greater multiplicity of the interband transitions, we expect the Van Vleck susceptibility to be very important - indeed it very likely dominates the total. A band calculation which explicitly computes the two components reckons the Pauli contribution at 15-20%, [34] in rough agreement with this multiplicity argument.

If \mathbf{H} is along the c-axis, then the relevant matrix element (with $\hbar = 1$) is:

$$|\langle \alpha | L_z + 2S_z | \beta \rangle|^2 = (36/49)j_z^2 \delta_{\alpha,\beta}. \quad (5.2)$$

At the Γ point, states of different j_z do not mix and the perturbation introduced by \mathbf{H} is diagonal. The occupation factors then imply that the Van Vleck susceptibility is zero for this direction. If \mathbf{H} is in the x -direction, the corresponding expression for the square of the matrix element is

$$|\langle \alpha | L_x + 2S_x | \beta \rangle|^2 = (36/49)(5/2 - j_z)(5/2 + j_z + 1) \quad (5.3)$$

if the states α and β differ by one unit of j_z and is zero otherwise. The Van Vleck susceptibility comes from four distinct pairs of states: $(j_z = -5/2, -3/2)$, $(-3/2, -1/2)$, $(1/2, 3/2)$ and $(3/2, 5/2)$, whenever one of the pair is occupied and the other unoccupied. The Pauli contribution to χ_{xx} , on the other hand, comes only from the pair $(-1/2, 1/2)$ when this state is occupied. A sheet of the Fermi surface will have an isotropic partial Pauli susceptibility ($\chi_{zz}^P/\chi_{xx}^P \approx 1$) if different j_z values are well mixed in the wavefunction, but will be anisotropic otherwise: $j_z=1/2$ implies $\chi_{zz}^P/\chi_{xx}^P \ll 1$, and $j_z=3/2$ or $j_z=5/2$ implies $\chi_{zz}^P/\chi_{xx}^P \gg 1$. As we shall see below, it is the anisotropy of the Pauli contribution which is critical for understanding the phase diagram. This means that the central question is: what is the j_z content of the Fermi surface, and how much mixing of different j_z 's is there? Band calculations give a clear answer to this question. They show that the parts of the Fermi surface near the Γ point and K point are predominantly $j_z=3/2$ or $5/2$, [35,36] while the parts near the A point are well mixed. This is illustrated in Fig. 7. Hence we expect a contribution to the Pauli susceptibility which satisfies $\chi_{zz}^P/\chi_{xx}^P \gg 1$ from the parts near Γ and K, representing roughly half the total density of states at the Fermi surface, and a contribution satisfying $\chi_{zz}^P/\chi_{xx}^P \approx 1$ for the rest of the Fermi surface. In treatments which go beyond band theory to discuss many-body renormalizations, it is found that the Pauli and Van Vleck parts are enhanced by similar factors [37].

Summing up these theoretical considerations, the magnetic susceptibility of UPt₃ is likely to be dominated by interband (Van Vleck) contributions. This is particularly true for χ_{xx} , which means that the anisotropy in the observed susceptibility ($\chi_{xx} > \chi_{zz}$) most likely stems from interband contributions. The Pauli susceptibility, on the other hand, is more likely to satisfy the opposite inequality $\chi_{xx}^P < \chi_{zz}^P$.

Experimentally, it is not easy to distinguish the Pauli and Van Vleck contributions to the susceptibility. The most straightforward way, in principle, is to measure the imaginary part of the susceptibility with neutron scattering. The Van Vleck contribution has a gap at low frequencies, while the Pauli part does not. For the present case, however, we also need to

distinguish the different components of the susceptibility tensor. This means that polarized beam experiments are required, with the associated lower counting rates. Finally, we are interested here in the uniform susceptibility, which means small-angle scattering. Thus this definitive experiment may be difficult to perform.

A more indirect but still informative test arises from the observation that the Pauli susceptibility depends on the density of states at the Fermi energy whereas the Van Vleck susceptibility depends on a joint density of states. The Pauli part is therefore directly comparable to C_V/T , where C_V is the specific heat. In this regard the peak in $\chi_{xx}(T)$ at $T=15$ K [30] (see Fig. 6) is of interest. This peak is absent in the smooth curve for $\chi_{zz}(T)$, and in the the specific heat $C_V(T)$, [31] This is consistent with the idea that the physical origins of χ_{zz} and χ_{xx} are different, and that the density of states at the Fermi level largely determines χ_{zz} but not χ_{xx} . Thus experiments, to the extent that we have them, confirm the theoretical picture.

The importance of these considerations for the superconducting state is simple. [38] Superconductivity affects the Pauli susceptibility in a drastic fashion. For a singlet state such as E_{1g} , the Pauli term $\chi_{ij}^P(T)$ is reduced to zero at zero temperature because it takes a finite amount of energy to break a pair and magnetize the system. Superconductivity should have no effect at all on the Van Vleck term, and conversely. The difference in free energies between the normal and superconducting states in a field is

$$F_{magnetic} = -\frac{1}{2} \sum_{ij} \Delta\chi_{ij}^P H_i H_j. \quad (5.4)$$

Here $\Delta\chi_{ij}^P = \chi_{ij}^S - \chi_{ij}^N$ where χ_{ij}^S and χ_{ij}^N are the Pauli susceptibilities in the superconducting and normal states, respectively. Just below the superconducting transition we know that the change in the susceptibility is quadratic in $\boldsymbol{\eta}$. Hence we add to the usual superconducting free energy the last three terms of Eq. 3.1 which are quadratic in both $\boldsymbol{\eta}$ and H .

From the arguments above we expect that a_x and a_d will be smaller than a_z since we anticipate that $\chi_{xx}^P < \chi_{zz}^P$. From our fits to the phase diagrams for the two directions of the field we find that a_z is slightly more than twice $a_x + a_d$, in agreement with the physical picture of the susceptibility. The differences in the sizes of the a terms affect what happens to the upper critical field curves for the two directions of the field at high fields. At high fields the Pauli limiting terms in the free energy, which are proportional to H^2 , dominate over the rest of the free energy, which gives a contribution to H_{c2} proportional to H . Because $a_z > a_x + a_d$, H_{c2} when the field is along the c-axis curves down more than H_{c2} when the field is in the basal plane. Consequently, the two upper critical field curves for the two directions cross. This crossing is shown in Fig. 8. We have therefore shown that the objection to the E_{1g} model on the grounds that it cannot explain the crossing of the upper critical field curves is invalid.

VI. PRESSURE EFFECTS

We have offered a comprehensive description of the phase diagram of Upt_3 in the $H - T$ plane. However, because of the rather large number of parameters in the Ginzburg-Landau free energy, this analysis is not yet sufficient to distinguish the E_{1g} picture from

competing pictures such as the E_{2u} picture and mixed representation pictures. Consideration of pressure effects will allow us to do this. We will show that only E_{1g} is consistent with these experiments. The analysis in this section is an elaboration of earlier work. [39] It is somewhat surprising that pressure experiments are so crucial for understanding the symmetry of the order parameter. Under normal circumstances, accessible pressures have only a small effect on superconducting parameters and qualitative conclusions are difficult to draw. In the present case, however, moderate pressures destroy antiferromagnetism, which restores the full hexagonal symmetry of the crystal structure. It is this singularly fortunate circumstance which makes pressure such a very powerful tool in unraveling the order parameter symmetry.

Qualitatively, the facts are these. The magnetization disappears at a critical pressure of about 3 kbar. The splitting in T_c also disappears at the same pressure. This shows that it is indeed the magnetization which splits the transition, as originally predicted [7]. The coincidence of the pressures at which these events take place rules out mixed representation theories such as the A-B theory [18]. In such theories the original splitting is due to an accidental degeneracy and is not related to the magnetization.

Our aim is to understand quantitatively the phases of UPt₃ in the entire (H, P, T) space. However, in order to understand the restoration of crystal symmetry, we first focus on the $(H = 0, P, T)$ plane, so that complications due to the gradient terms can be treated separately. The expression for the free energy density of the coupled magnetic-superconducting system is then $f = f_S + f_M + f_{SM}$, where

$$f_M = \alpha_M(P, T)M^2 + \beta_M M^4 \quad (6.1)$$

$$f_S = \alpha_S(P, T)\boldsymbol{\eta} \cdot \boldsymbol{\eta}^* + \beta_1(\boldsymbol{\eta} \cdot \boldsymbol{\eta}^*)^2 + \beta_2|\boldsymbol{\eta} \cdot \boldsymbol{\eta}|^2 \quad (6.2)$$

$$f_{SM} = b|\mathbf{M} \cdot \boldsymbol{\eta}|^2 + b'M^2\boldsymbol{\eta} \cdot \boldsymbol{\eta}^* \quad (6.3)$$

We have assumed, as is conventional, that the pressure dependence of fourth-order coefficients is weak and can be neglected.

f_M , the magnetic part of the free energy, entirely determines the behavior of the magnetization above T_{c1} . (Recall that T_{c1} is the higher of the two observed transition temperatures.) The experimental data from neutron scattering measurements of M^2 (proportional to the magnetic Bragg scattering at the $(1, \frac{1}{2}, 0)$ point) are sufficient to determine the parameters. At $P = 0$ and $T > T_{c1} = 0.5$ K, M^2 is a linear function of $T_N - T$, where $T_N = 5$ K is the Neel temperature. [8,40] One finds $\alpha_M(P = 0, T)/\beta_M = (1.6 \times 10^{-4} \mu_B^2/\text{K})(T - T_N)$.

As to the P dependence, it is found that T_N is nearly independent of pressure from $P = 0$ to $P = 2$ kbar and that $M^2 \sim (P_N - P)$ for $T < 2$ K [40], where $P_N \approx 3$ kbar is the critical pressure at which magnetism disappears. From the point of view of this paper, which concentrates on the superconducting regime $T < T_{c1}$, we may therefore take $\alpha_M = \alpha_M^0(P - P_N)(T - T_N) \approx -\alpha_M^0 T_N (P - P_N)$, where $\alpha_M^0/\beta_M = 5.3 \times 10^{-5} \mu_B^2/\text{K-kbar}$. Note that this value and the coefficient of the expression for $\alpha_M(P = 0, T)/\beta_M$ have been corrected from an earlier paper written by one of us (Joynt) [39].

The pressure dependence of $\alpha_S(P, T)$ may be obtained if we assume that $\alpha_S(P, T) = \alpha_{ST}(T - T_c^0) + \alpha_{SP}P$, so that $\alpha_S(P, T)$ is a linear function of P . $\alpha_{ST}(T)$ is the zero pressure

value of $\alpha_S(P, T)$ which has already been determined. For $P > P_N$, $M = 0$ and the pressure dependence of T_c is entirely due to the coefficient α_{SP} . Since $dT_c/dP = -11$ mK/kbar in this region [41], we find $\alpha_{SP} = \alpha_{ST}(11 \text{ mK/kbar})$.

At $P = 0$ and $T < T_{c1}$, there is a competition between the purely magnetic terms and the coupling term f_{SM} . Because $\boldsymbol{\eta} \cdot \boldsymbol{\eta}^* \sim T_{c1} - T$ for $T < T_{c1}$ and $\boldsymbol{\eta} = 0$ for $T > T_{c1}$, the coupling term predicts that \mathbf{M} should have a kink at T_{c1} . The magnitude of the kink may easily be computed using Eqs. 6.1, 6.2, 6.3. Differentiation leads to two linear equations for M and $\boldsymbol{\eta} = \eta \hat{\mathbf{x}}$

$$\eta^2 = [\alpha_S(T_c^0 - T) - (b + b')M^2]/2(\beta_1 + \beta_2) \quad (6.4)$$

$$M^2 = [\alpha_M(T_N - T) - (b + b')\eta^2]/2\beta_M, \quad (6.5)$$

which give the behavior of the order parameters below T_{c1} . Above T_{c1} we have simply

$$M^2 = \alpha_M(T_N - T)/2\beta_M \quad (6.6)$$

The slope is discontinuous at T_{c1} :

$$\left[1 - \frac{(b + b')^2}{4\beta_M(\beta_1 + \beta_2)} \right] \frac{dM^2}{dT} \Big|_{T < T_{c1}} = \frac{dM^2}{dT} \Big|_{T > T_{c1}} + \frac{\alpha_{ST}(b + b')}{4\beta_M(\beta_1 + \beta_2)}. \quad (6.7)$$

If we take the approximation that the coupling $(b + b')$ is small, then we may write the discontinuity as

$$\Delta \frac{dM^2}{dT} = - \frac{\alpha_{ST}(b + b')}{4\beta_M(\beta_1 + \beta_2)}. \quad (6.8)$$

In these formulas $\boldsymbol{\eta}$ is assumed to be parallel to \mathbf{M} . If these two vectors are perpendicular, then b should appear instead of $(b + b')$. The kink is observed experimentally, [8] which again confirms that the splitting of the superconducting transition is due to f_{SM} . These formulas assume that there is only one component of \mathbf{M} , contrary to the idea of Blount *et al.* [23] that the moment rotates at T_{c1} . Recent experiments have indeed ruled out the possibility of rotation [42].

We now wish to calculate the phase diagram at finite pressures, assuming that the only pressure dependence comes from α_S and α_M . All other parameters are taken to have their zero pressure values. The only dependence on pressure in our theory of the phase diagram is through the quantity ΔT . We calculate ΔT at various pressures by taking $T_x(P = 0)$ and $T_y(P = 0)$ from our zero pressure fit, dT_y/dP (recall $T_y > T_x$), P_N and dT_c/dP (for $P > P_N$) from experimental data [41]. From $T_x(P = 0)$ and P_N we can then find dT_x/dP . In Fig. 9 we plot the phase diagram in the $H - T$ plane at various pressures for \mathbf{H} in the basal plane using the renormalized Q_x (see section III). The behavior with pressure is easily understood qualitatively. The main effect of pressure is to close up the splitting of the zero-field critical temperatures. Thus the tetracritical point moves down toward the T -axis and disappears, as does the A (low field, high temperature) phase. Thus the C (high field, low temperature) - B (low field, low temperature) phase boundary is very sensitive to pressure as it ends

at the tetracritical point. This is observed experimentally. [43] On the other hand, the N (normal state) - C boundary (upper part of the H_{c2} curve) is not very sensitive to pressure. Again, the agreement between theory and experiment is very satisfactory. It is difficult to compare these predictions with the three-dimensional phase diagram of Boukhny *et al.* [44] quantitatively. The pressure dependence of the critical temperatures given by these authors is not in good agreement with that of Trappmann *et al.* [41], which we used in plotting the figures. The behavior of the boundaries is quite sensitive to this dependence. Nevertheless there appears to be very satisfactory qualitative agreement between theory and experiment, with one exception. The experiment shows that there is an additional phase boundary in the P - T plane when $P > P_N$. This cannot be a pure superconducting transition in a two-component theory. We believe this to be a mixed magnetic-superconducting transition, so that this boundary is essentially an extension of the magnetic phase boundary. The signal in the sound velocity is very small. It may be larger than in the normal phase because of the coupling to the superconducting order parameter which is serving as a secondary order parameter in the transition.

Let us compare this behavior to the behavior of the phase boundaries in the E_{2u} theory in which $K_2 \approx K_3 \approx 0$. The best fit with this constraint is given in Fig. 10. This picture is in qualitative disagreement with experiment. Again, the qualitative reason for this is easily understood. In the E_{2u} theory, the difference in slope between the H_{c2} curves for η_x and η_y is due only to their differing energies in the presence of the magnetization. Once $P > P_N$, this difference is gone and the two components have identical free energies and identical slopes. The E_{2u} theory says that the N-A and A-B boundaries must move together, not apart, under the influence of pressure. This is in conflict with experiment.

VII. CONCLUSION

The Ginzburg-Landau theory is a very powerful tool in the physics of unconventional superconductivity. We have pushed the theory to obtain as much information as possible about the phase diagram. Mathematical difficulties arise when a magnetic field is applied, a circumstance which has made the theory of the phase diagram of UPt₃ proceed more slowly than might have been expected. The method of classifying terms according to their behavior in the effective field appears to have solved the linear problem in principle, though explicit calculations for a general direction of the field still appear daunting. We have limited our treatment to the two high symmetry field directions. Most experiments are also limited to these directions.

Consistent application of the method, taking into account the Pauli-limiting effect, gives very good agreement between theory and experiment for the E_{1g} theory. It would be desirable, however, to have an explicit calculation of the nonlinear renormalization factors entering the repulsion of the phase boundaries; obtaining this by a fit, as done here, is not truly satisfactory from the theorist's point of view. The peculiar phenomenon of the H_{c2} crossing is interpreted here as arising from an interplay of intraband Pauli magnetism and interband Van Vleck magnetism. While the picture of the anisotropic susceptibility which emerges is a natural one, it would be good to have some independent confirmation of it.

The surprise of the past several years is that pressure experiments have been able to play

a critical role in sorting out the nature of the order parameter. They have demonstrated that it is the magnetism which splits the critical temperature. Above the critical pressure, the hexagonal symmetry is restored. Experiments above this pressure have shown that there are still two phase transitions as a function of field - this means that the field direction itself couples to the internal degrees of freedom in the two-component order parameter. This only occurs in the E_{1g} picture, which appears to be the only choice fully consistent with all experiments.

We would like to acknowledge useful discussions and correspondence with M. Norman, A. Garg, and particularly D. Cox. This work was supported by the National Science Foundation through grant no. DMR-9214739.

REFERENCES

- [1] R. Fisher, S. Kim, B. Woodfield, N. Phillips, L. Taillefer, K. Hasselbach, J. Flouquet, A. Giorgi, and J. L. Smith, *Phys. Rev. Lett.* **62**, 1411 (1989).
- [2] K. Hasselbach, L. Taillefer, and J. Flouquet, *Phys. Rev. Lett.* **63**, 93 (1989).
- [3] G. Bruls, B. Wolf, P. Thalmeier, B. Lüthi, A. de Visser, and A. Menovsky, *Phys. Rev. Lett.* **65**, 2294 (1990).
- [4] Y. Qian, M. Xu, A. Schenstrom, H. Baum, J. Ketterson, D. Hinks, M. Levy, and B. Sarma, *Sol. State Comm.* **63** 599 (1987).
- [5] S. Adenwalla, S. W. Lin, Q. Z. Ran, Z. Zhao, J. B. Ketterson, J. A. Sauls, L. Taillefer, D. G. Hinks, M. Levy, and Bimal K. Sarma, *Phys. Rev. Lett.* **65**, 2298 (1990).
- [6] S.-W. Lin, C. Jin, H. Zhang, J. B. Ketterson, D. M. Lee, D.G. Hinks, M. Levy, and Bimal K. Sarma, *Phys. Rev. B* **49**, 10 001 (1994). The sound experiments are reviewed in B. K. Sarma, M. Levy, S. Adenwalla, and J. Ketterson, *Physical Acoustics, vol. 20*, (Academic Press, New York, 1992), p. 107
- [7] R. Joynt, *Supercond. Sci. Technol.* **1**, 210 (1988).
- [8] G. Aeppli, E. Bucher, C. Broholm, J. K. Kjems, J. Baumann and J. Hufnagl, *Phys. Rev. Lett.* **60**, 615 (1988).
- [9] D. W. Hess, T. A. Tokayasu, and J. A. Sauls, *J. Phys.: Condens. Matter* **1**, 8135 (1989).
- [10] K. Machida and M. Ozaki, *J. Phys. Soc. Japan* **48**, 2244 1989
- [11] Manfred Sigrist and Kazuo Ueda, *Rev. Mod. Phys.* **63**, 239 (1991). In the present work, we follow the notation established by this review article.
- [12] G. E. Volovik and L. P. Gorkov, *Zh. Eksp. Teor. Phys.* **88**, 1412 (1985) [*Sov. Phys. JETP* **61**, 843 (1985)].
- [13] B. S. Shivaram, Y. Jeong, T. Rosenbaum, and D. Hinks, *Phys. Rev. Lett.* **56**, 1078 (1986).
- [14] P. Hirschfeld, D. Vollhardt, and P. Wölfle, *Sol. St. Comm.* **59**, 111 (1986).
- [15] B. Lussier, B. Ellmann, and L. Taillefer, *Phys. Rev. Lett.* **73** 3294 (1994).
- [16] E. I. Blount, *Phys. Rev. B* **32**, 2935 (1985).
- [17] J. A. Sauls, *Adv. in Phys.* **43**, 113 (1994).
- [18] A. Garg, *Phys. Rev. Lett.* **69**, 676 (1992).
- [19] B. Shivaram, T. Rosenbaum, and D. Hinks, *Phys. Rev. Lett.* **57**, 1259 (1986).
- [20] C. Choi and J. Sauls, *Phys. Rev. Lett.* **66**, 484 (1991).
- [21] R. Joynt, *Europhys. Lett.* **16**, 289 (1991).
- [22] M.E. Zhitomirskii, *Pis'ma Zh. Eksp. Teor. Fiz.* **49**, 333 (1989) [*JETP Lett.* **49**, 379 (1989)].
- [23] E. I. Blount, C. M. Varma, and G. Aeppli, *Phys. Rev. Lett.* **64**, 3074 (1990).
- [24] M. Sigrist, R. Joynt, and T. M. Rice, *Phys. Rev. B* **36**, 5186 (1987).
- [25] I. Luk'yanchuk and V. Mineev, *Zh. Eksp. Teor. Fiz.* **93**, 2045 (1987) [*Sov. Phys. JETP* **66**, 2045 (1987)].
- [26] D. Chen and A. Garg, *Phys. Rev B* **49**, 479 (1994).
- [27] K. Hasselbach, A. Lacerda, K. Behnia, L. Taillefer, J. Flouquet, and A. de Visser, *J. Low Temp. Phys.* **81**, 299 (1990).
- [28] S.K. Sundaram and R. Joynt, *Phys. Rev. B* **40**, 8780 (1989).

- [29] C. Choi and P. Muzikar, Phys. Rev B **40**, 5144 (1989); M. Palumbo, C. H. Choi, and P. Muzikar, Physica B **165-166**, 1095 (1990).
- [30] P. Frings, J. Franse, F. deBoer, and A. Menovsky, J. Magn. Magn. Mater. **31**, 240 (1983).
- [31] A. de Visser, A. Menovsky, and J. Franse, Physica B **147**, 81 (1987).
- [32] C.S. Wang *et al.*, Phys. Rev. B **35**, 7260 (1987).
- [33] V. L. Líbero and D. L. Cox, Phys. Rev. B **48**, 3783 (3783).
- [34] M.R. Norman, T. Oguchi, and A.J. Freeman, Phys. Rev. B **38**, 11193 (1988).
- [35] G. Zwicknagl, J. Magn. Magn. Mater. **76-77**, 16 (1988).
- [36] N. Christensen, O. Andersen, O. Gunnarson, and O. Jepsen, *ibid.* **76-77**, 23 (1988).
- [37] F. C. Zhang and T. K. Lee, Phys. Rev. Lett. **58**, 2728 (1987); C. Varma and G. Aeppli, *ibid.* **58**, 2729 (1987); D. L. Cox, *ibid.* **58**, 2730 (1987).
- [38] This points made in this paragraph have been stressed particularly by D. L. Cox (private communication).
- [39] R. Joynt, Phys. Rev. Lett. **71**, 3015 (1993).
- [40] S. Hayden, L. Taillefer, C. Vettier, and J. Flouquet, Phys. Rev. B **46**, 8675 (1992).
- [41] T. Trappmann, H. v. Löhneysen, and L. Taillefer, Phys. Rev. B. **43**, 13714 (1991); H. v. Löhneysen, T. Trappmann, and L. Taillefer, J. Magn. Magn. Mater. **108**, 49 (1992).
- [42] G. Luke *et al.*, (unpublished).
- [43] N. van Dijk, A. de Visser, J. Franse, S. Holtmeier, L. Taillefer, and J. Flouquet, Phys. Rev. B **48**, 1299 (1993), and N. van Dijk, A. de Visser, J. Franse, L. Taillefer, J. Low Temp. Phys. **93**, 101 (1993).
- [44] M. Boukhny, G. Bullock, B. Shivaram, and D. Hinks, Phys. Rev. Lett. **73**, 1707 (1994).

FIGURES

FIG. 1. Consequences of the effective field in the s-wave case. (a) Eigenvalue curves for the original lattice with $k \in L$. The lines are the solutions to Eq. 2.14. However, all transitions are suppressed by the effective field except the original H_{c2} line. In the case of arrows, the repulsion of the boundary to unphysical values of H and T takes place. In the case of cross-hatching, the transition is converted to a crossover. The numbers in parentheses denote the class of the line. (b) Curves for the new lattice with $k \in L'$. As in (a), except that the new lattice interpenetrates the old one. All lines are repelled by the effective field, and the C_{nk} corresponding to these boundaries never become nonzero.

FIG. 2. Consequences of the effective field in the d-wave case. (a) Eigenvalue curves for the original lattice with $k \in L$ setting the eigenvalues of the quadratic form in Eq. 2.28 equal to zero, neglecting the fourth-order terms. Most transitions are converted to crossovers by the effective field except the original H_{c2} line. The numbers in parentheses denote the class of the line. (b) New lattice with $k \in L'$. As in (a), but the new lattice interpenetrates the old one. Transitions corresponding to C_{0a} and C_{0b} are repelled only a short distance (single arrows). The dashed lines show the final positions of these boundaries after taking into account the effective field. A single internal transition line remains.

FIG. 3. The flux lattice for η_y . The filled circles indicate the singularities in the flux lattice. The Wigner-Seitz primitive unit cell is indicated by the dashed line. Its basis vectors are also shown. The integral I_2 ($|I_2| = |\langle (\eta_x^*)^2 \eta_y^2 \rangle|$) is non-zero only if the singularities in the η_x flux lattice are located at the b (open square), c (open oval) or d point (x), or one of the symmetrically equivalent points. These points for the b (c) point are the filled squares (filled oval). The axes are $\bar{z} = z/\ell$ (\parallel c-axis) and $\bar{y} = y/\ell$. The diagram is drawn to scale using the values of the parameters we obtain through our fits. The flux lattice for η_x is identical except for greater elongation in the \bar{z} direction.

FIG. 4. Phase diagram when the field is in the basal plane. The data points are from ultrasonic velocity measurements and are taken from Ref. [5], Fig. 3. The solid lines are our fit without the renormalization discussed in the text. The dashed line corresponds to a renormalization of Q_x by 2.67 or $\tilde{Q}_x = 2.67Q_x$. The constants used to make these graphs are $T_x = 0.458$ K, $T_y = 0.504$ K, $S_{c2x} = -9.26$ T/K, $S_{c2y} = -4.39$ T/K, $a_x/\alpha_0 = 0.0138$ K/T², and $a_d/\alpha_0 = 0.0193$ K/T²

FIG. 5. Phase diagram when the field is in the z -direction. The lines are the theoretical fits to H_{c2} (solid line) and the inner transition (dashed line). The data points are from ultrasonic velocity measurements and are taken from Ref. [5], Fig. 3. In addition to the constants used to make Fig. 4 we have used $\alpha_0/K_1 = 5.6 \times 10^{12}$ K⁻¹cm⁻², $\epsilon = 5.26 \times 10^{-5}$ G⁻¹, $a_z/\alpha_0 = 6.3 \times 10^{-10}$ K/G², and $(K_2 - K_3)/K_1 = 0.1$. We use $(K_2 + K_3)/K_1 = (S_{c2x}/S_{c2y})^2 - 1 + \hbar c \alpha_0 \epsilon \Delta T [(S_{c2x}/S_{c2y})^2 + 1] / (2eK_1)$ and $K_4/K_1 = [(1 + \alpha_0 \epsilon \Delta T / K_1) [2eK_1 S_{c2x} / (\hbar c \alpha_0)]^2]^{-1}$ to obtain $(K_2 + K_3)/K_1 = 1.0$ and $K_4/K_1 = 7.20$.

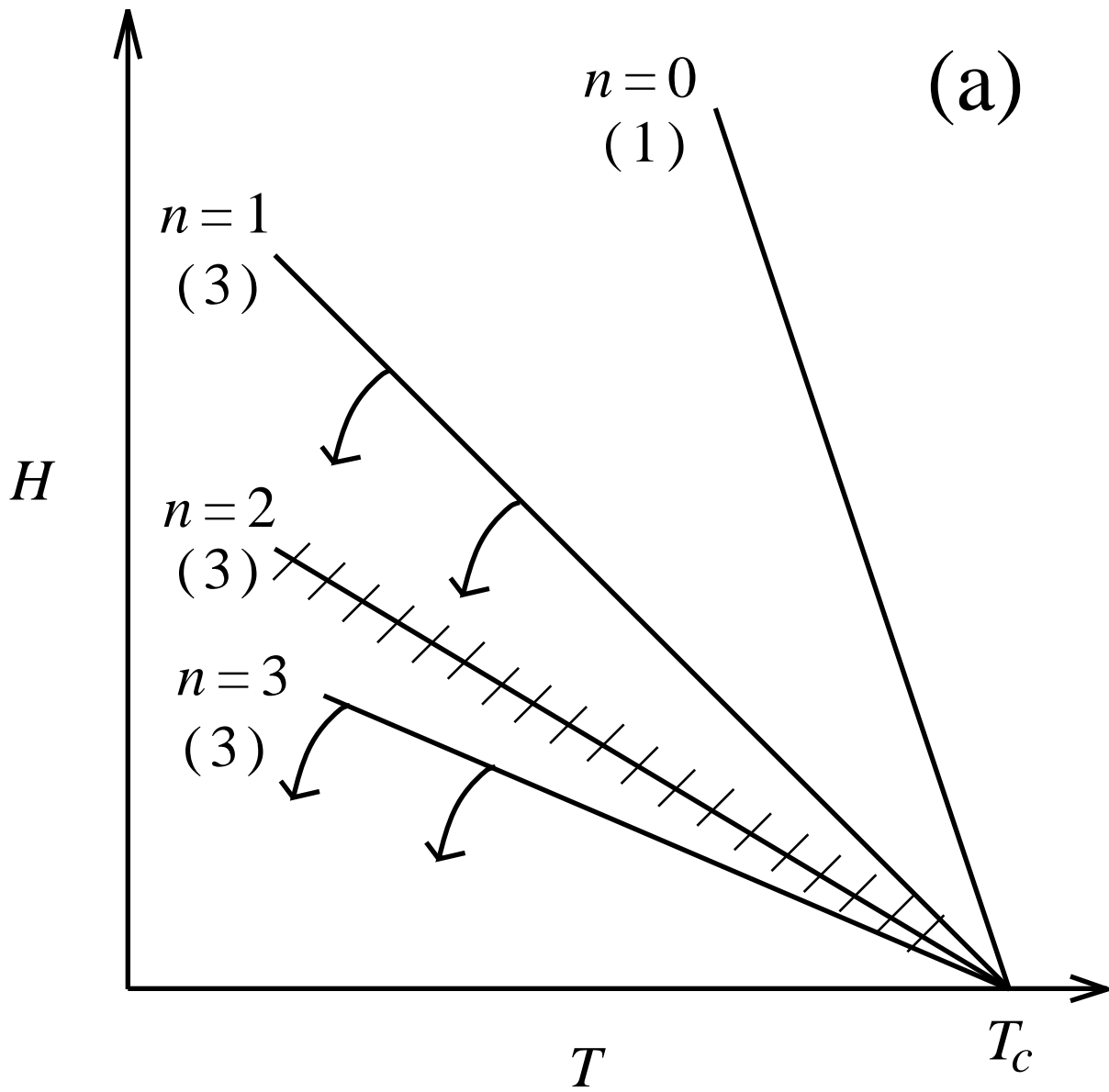
FIG. 6. Susceptibility of UPt_3 for fields oriented along the crystal's a-axis (circles), b-axis (triangles), and c-axis (squares). The graph is taken from Ref. [31], Fig. 2.1.

FIG. 7. Fermi surface of UPt_3 from Ref. [36], Fig. 5. The Fermi surface shown was calculated in the local density approximation using the Dirac-relativistic linear muffin-tin orbital method. The stripes show the j_z content of the Fermi surface: dotted for $|j_z| = 1/2$, right-hatched (///) for $|j_z| = 3/2$, and left-hatched for $|j_z| = 5/2$. The $|j_z| = 7/2$ component is small over the entire Fermi surface. Note that the parts of the Fermi surface around the Γ and K points are predominantly $|j_z| = 3/2$ or $5/2$, while the parts around the A point have well-mixed $|j_z|$'s. Fig. 2(b) of Ref. [35] is similar.

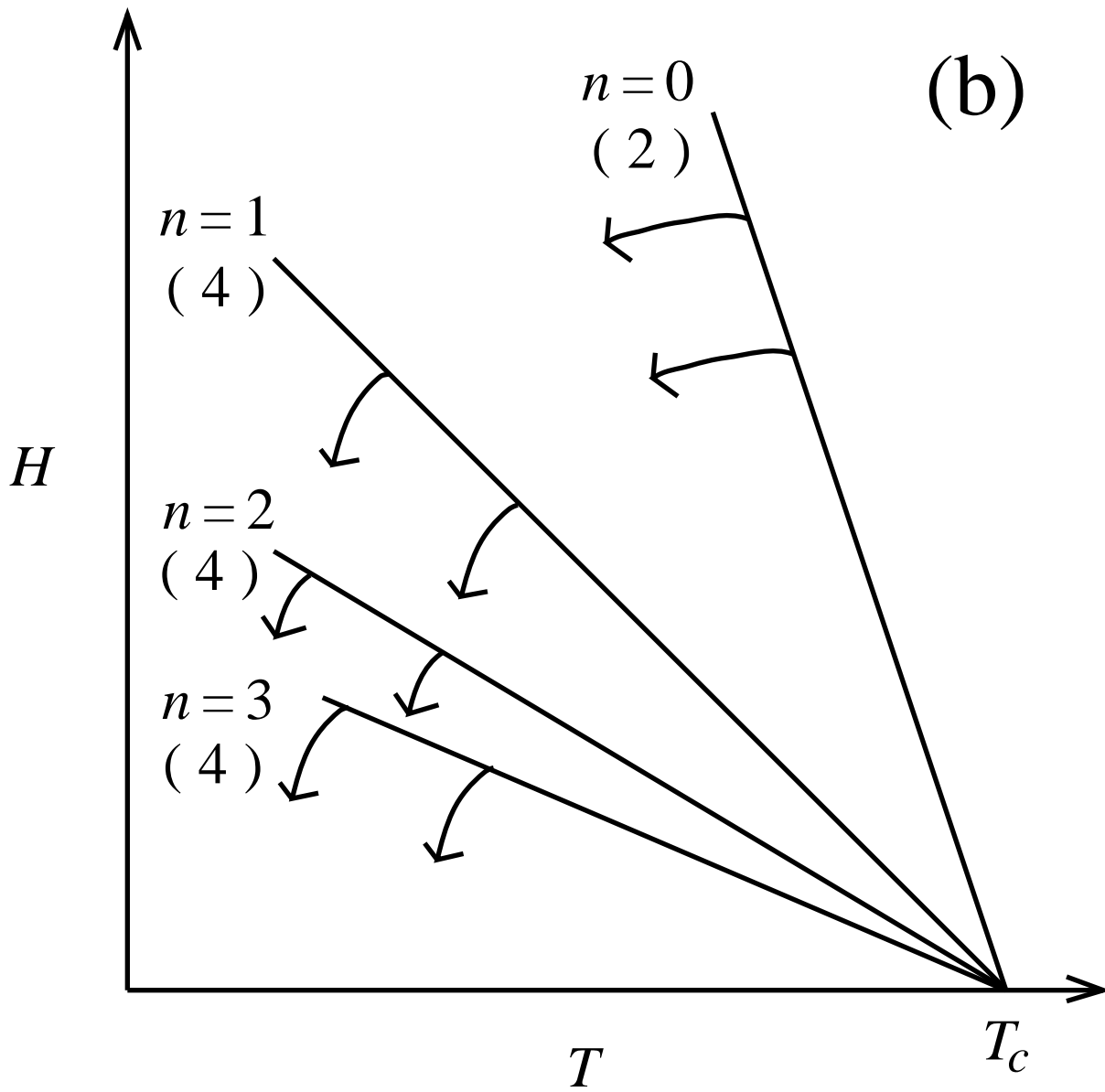
FIG. 8. The crossing of the H_{c2} line when the field is the basal plane (solid line) and the H_{c2} line when the field is in the z -direction (dashed line). The data points are from ultrasonic velocity measurements and are taken from Ref. [5], Fig. 3. The diamonds are for the case when the field is in the basal plane ($\mathbf{H} \parallel ab$) and the crosses are for the case when the field is in the z -direction ($\mathbf{H} \parallel c$).

FIG. 9. Pressure dependence of the phase diagram with the field in the basal plane in the E_{1g} model. The phase diagram is plotted at pressures (P) of (a) $P = 0$, (b) $P = P_N/2$ (1.85 kbar), (c) $P = P_N$ (3.7 kbar), and (d) $P = (3/2)P_N$ (5.55 kbar). Here P_N is the pressure above which the temperature splitting vanishes. As discussed in the text the theoretical inner transition line for temperatures below the tetracritical point ($H_y^*(T)$) has been renormalized. The data points in (a) are taken from Ref. [5], Fig. 3. The variation of the transition temperatures with pressure is taken from Ref. [41].

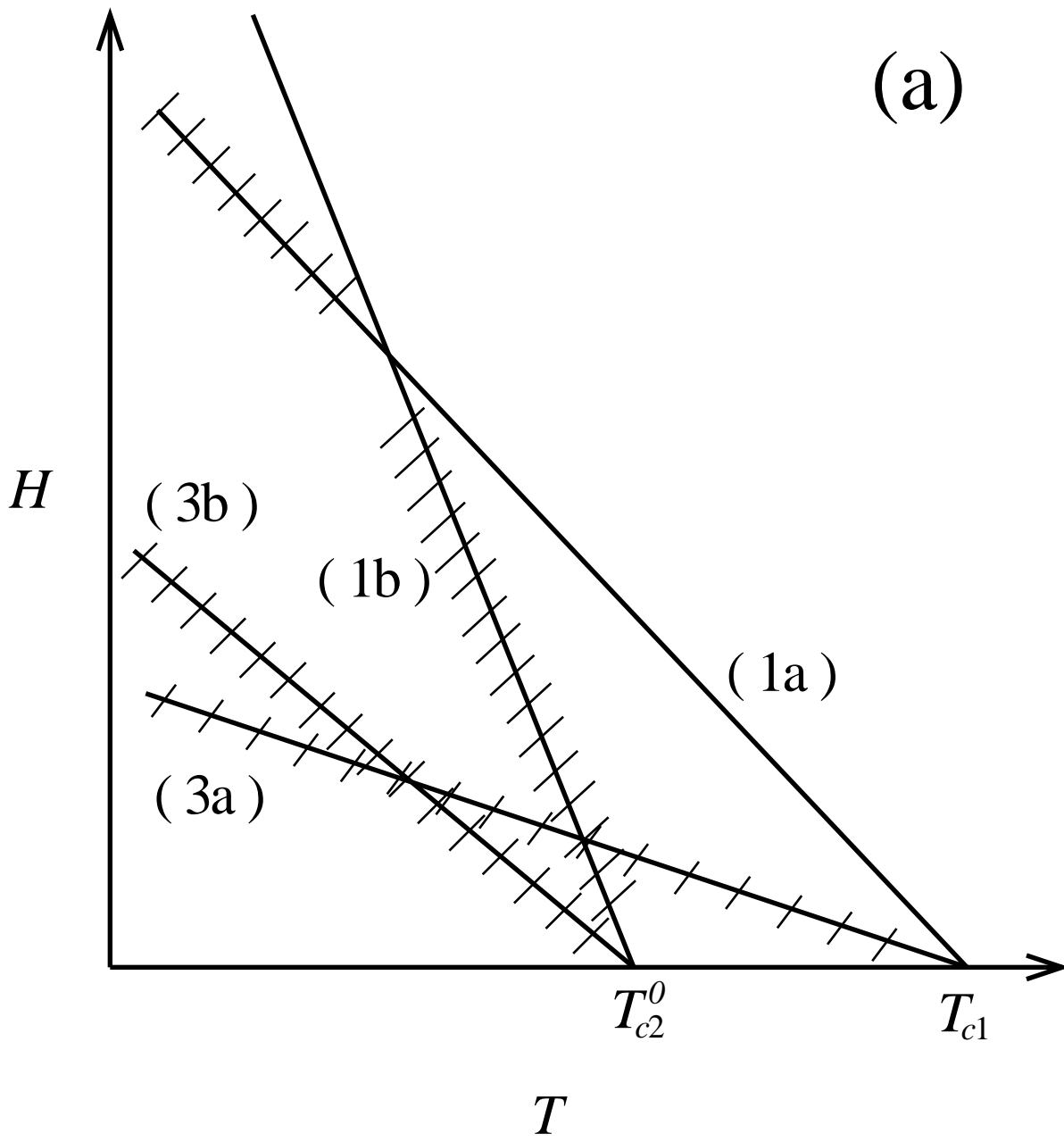
FIG. 10. Pressure dependence of the phase diagram with the field in the basal plane with $(K_2 + K_3)/K_1 = 0$ (E_{2u} model). The phase diagram is plotted at pressures (P) of (a) $P = 0$, (b) $P = (1/2)P_N$ (1.87 kbar), (c) $P = P_N$ (3.7 kbar), and (d) $P = (3/2)P_N$ (5.55 kbar). In order to obtain a better fit in this model we have changed the values of some of our input parameters. In these phase diagrams $a_x = a_d = 0$, $S_{c2x} = -6.66$ T/K, $S_{c2y} = -4.07$ T/K, $T_x = 0.465$ K, and $T_y = 0.509$ K. The data, renormalization of $H_y^*(T)$, and all other input parameters are the same as those for Fig. 9.



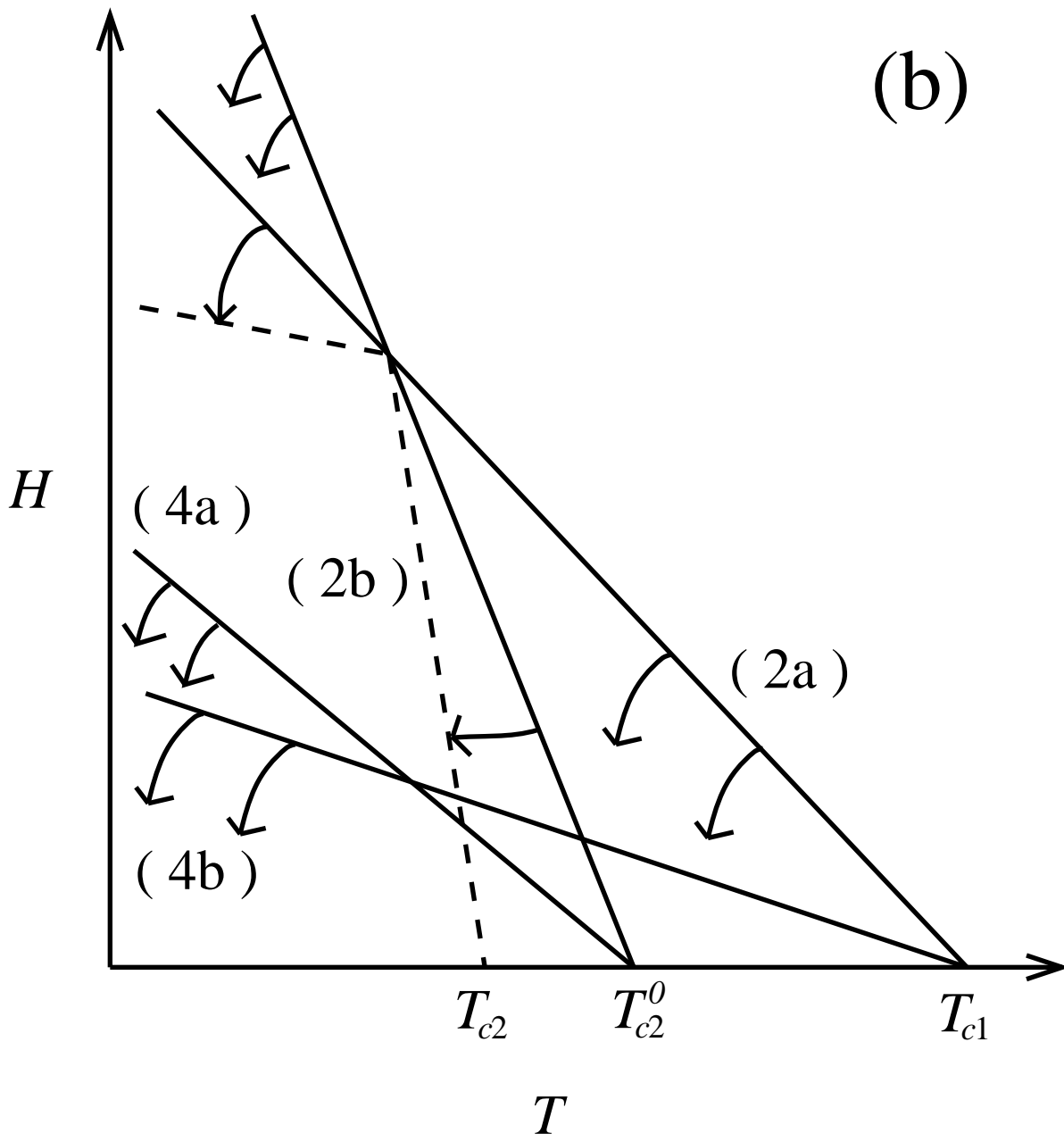
K. A. Park and Robert Joynt: Fig 1(a)



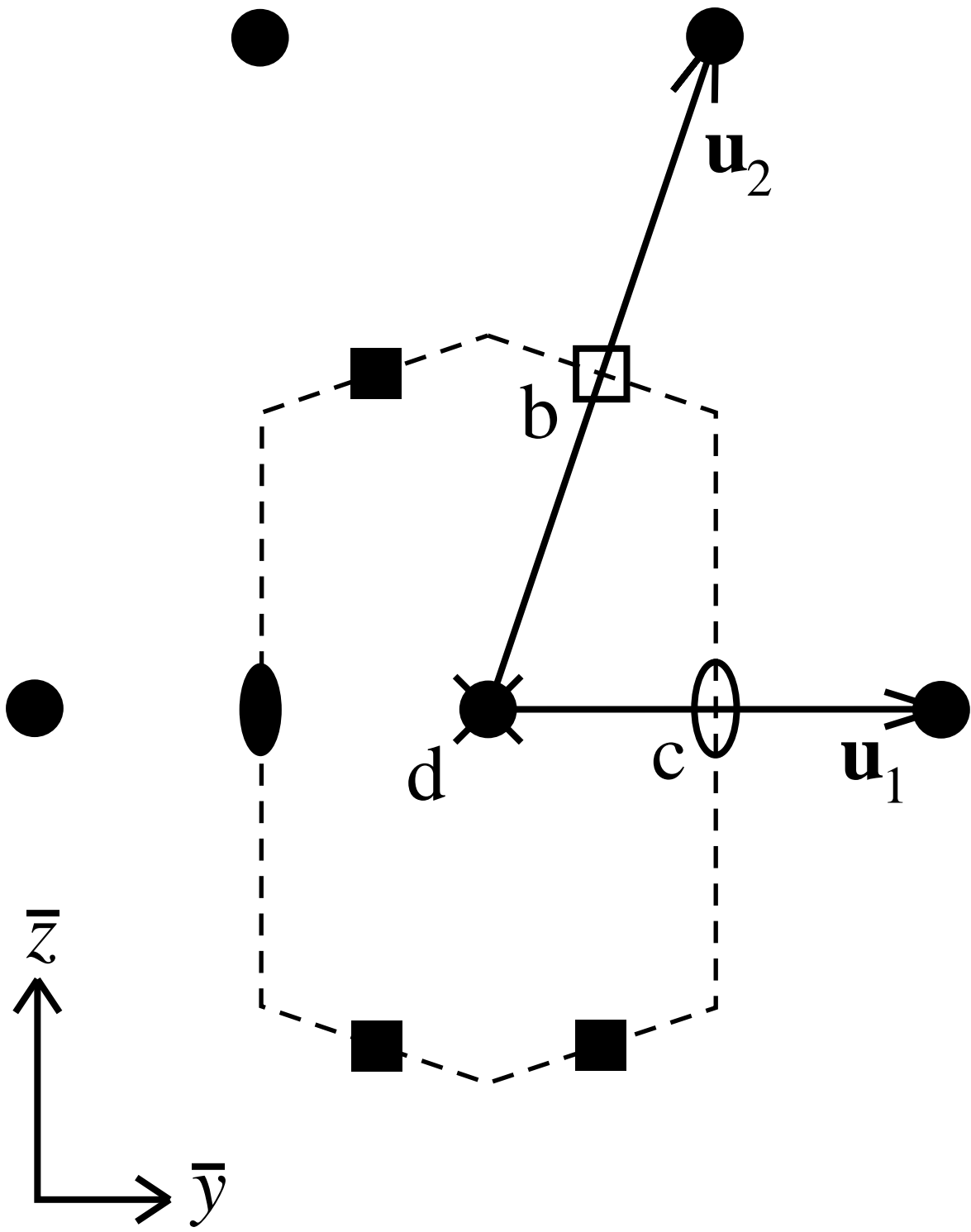
K. A. Park and Robert Joynt: Fig 1(b)



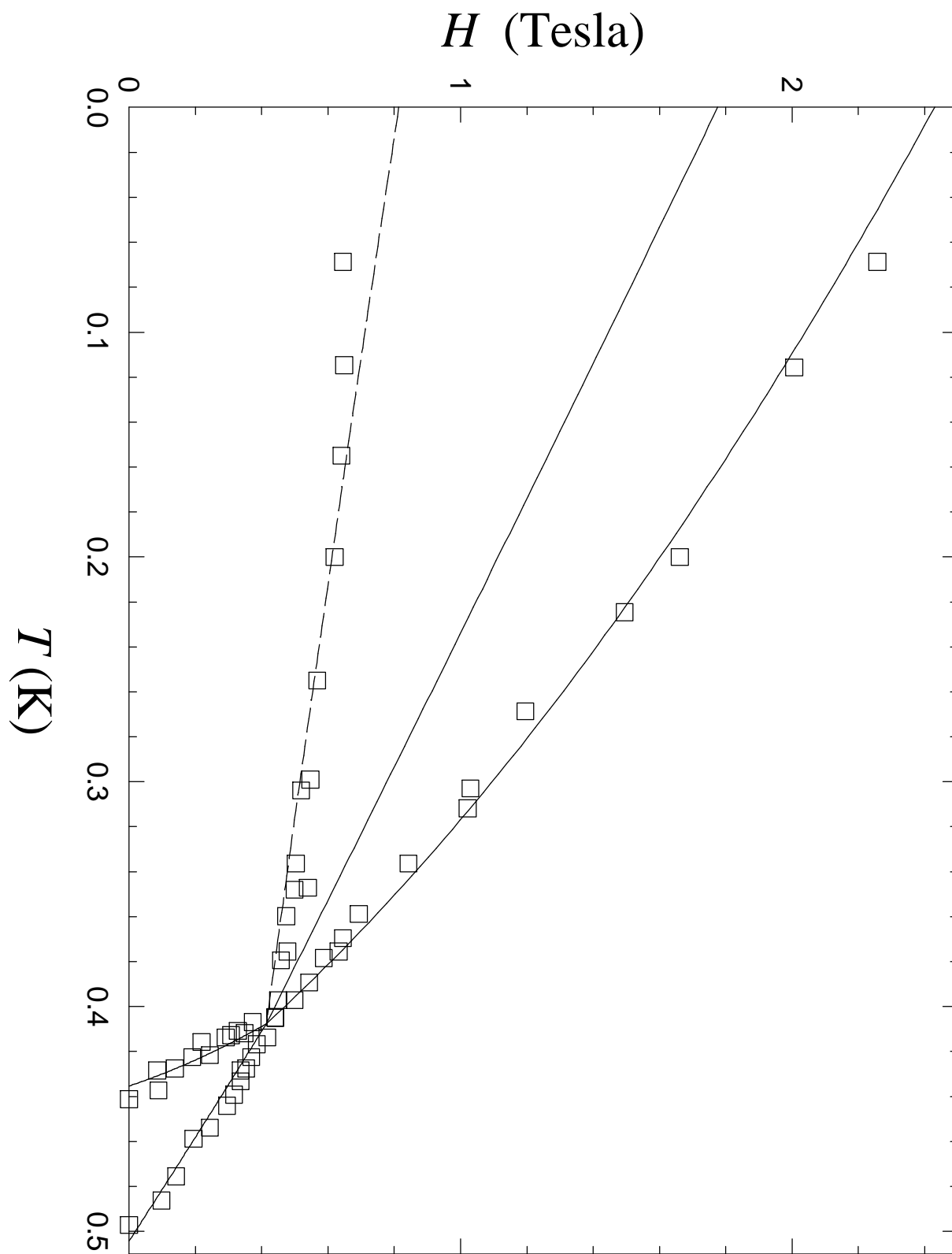
K. A. Park and Robert Joynt: Fig. 2(a)



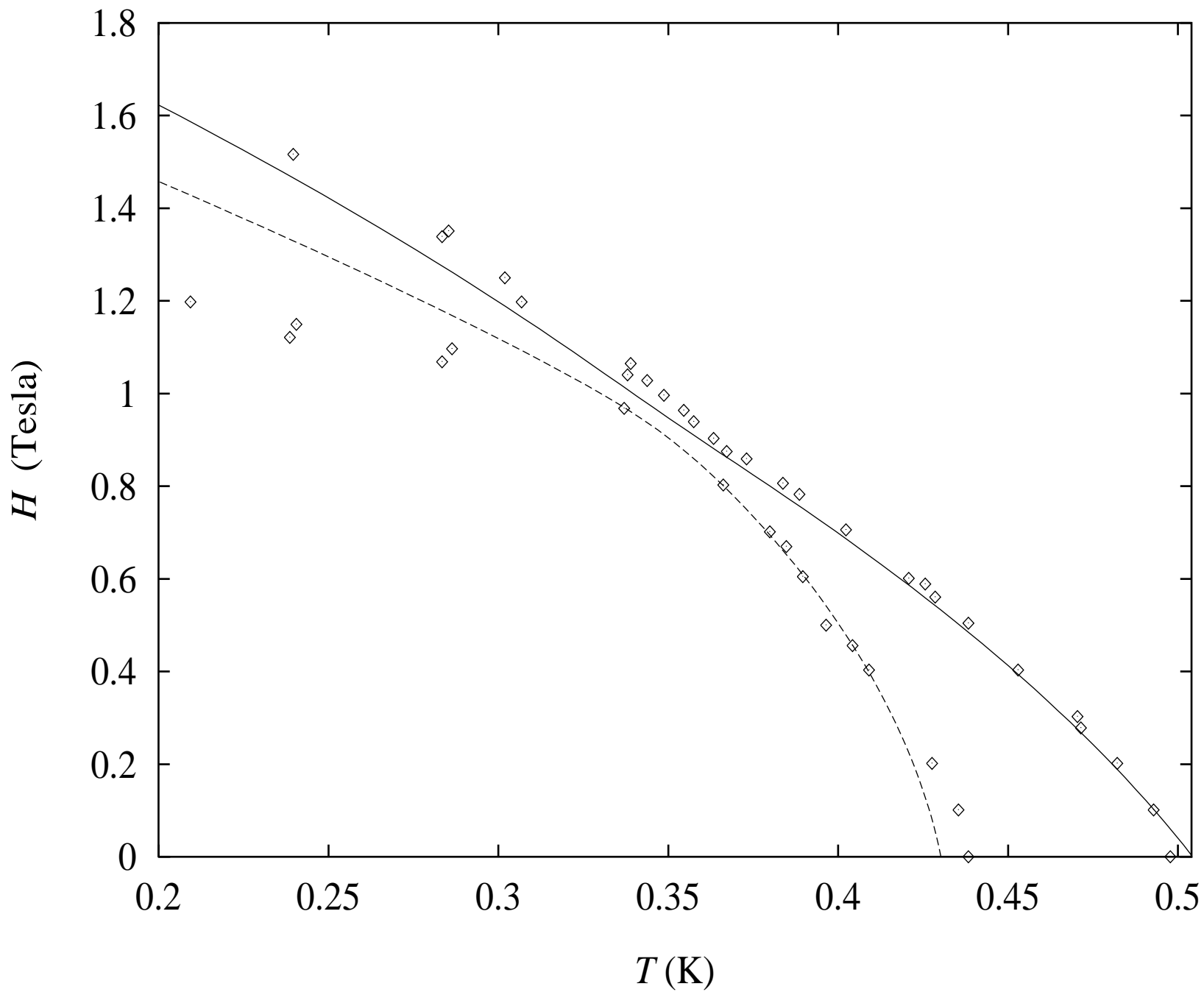
K. A. Park and Robert Joynt: Fig. 2(b)



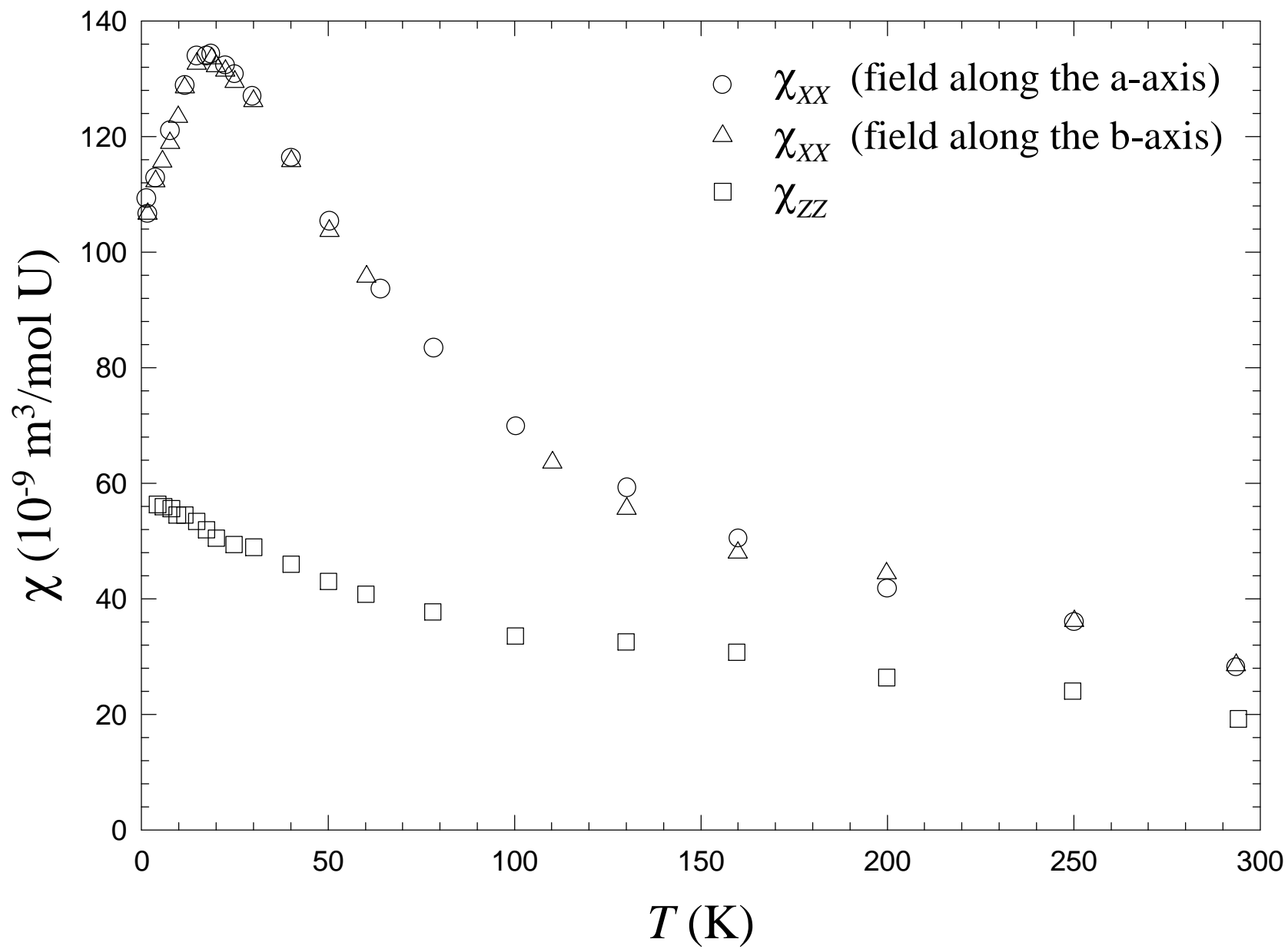
K. A. Park and Robert Joynt: Fig. 3



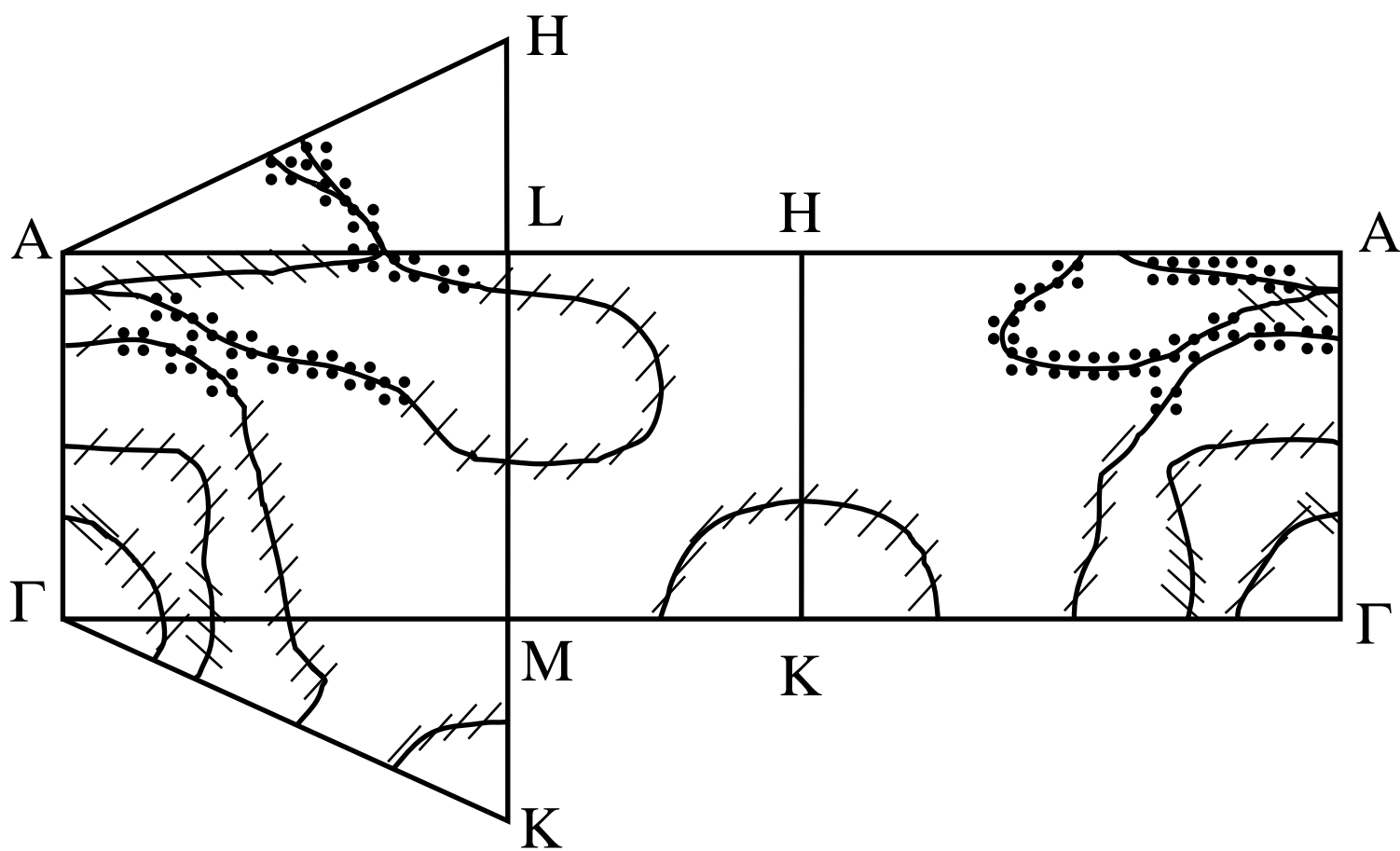
K. A. Park and Robert Joynt: Fig. 4



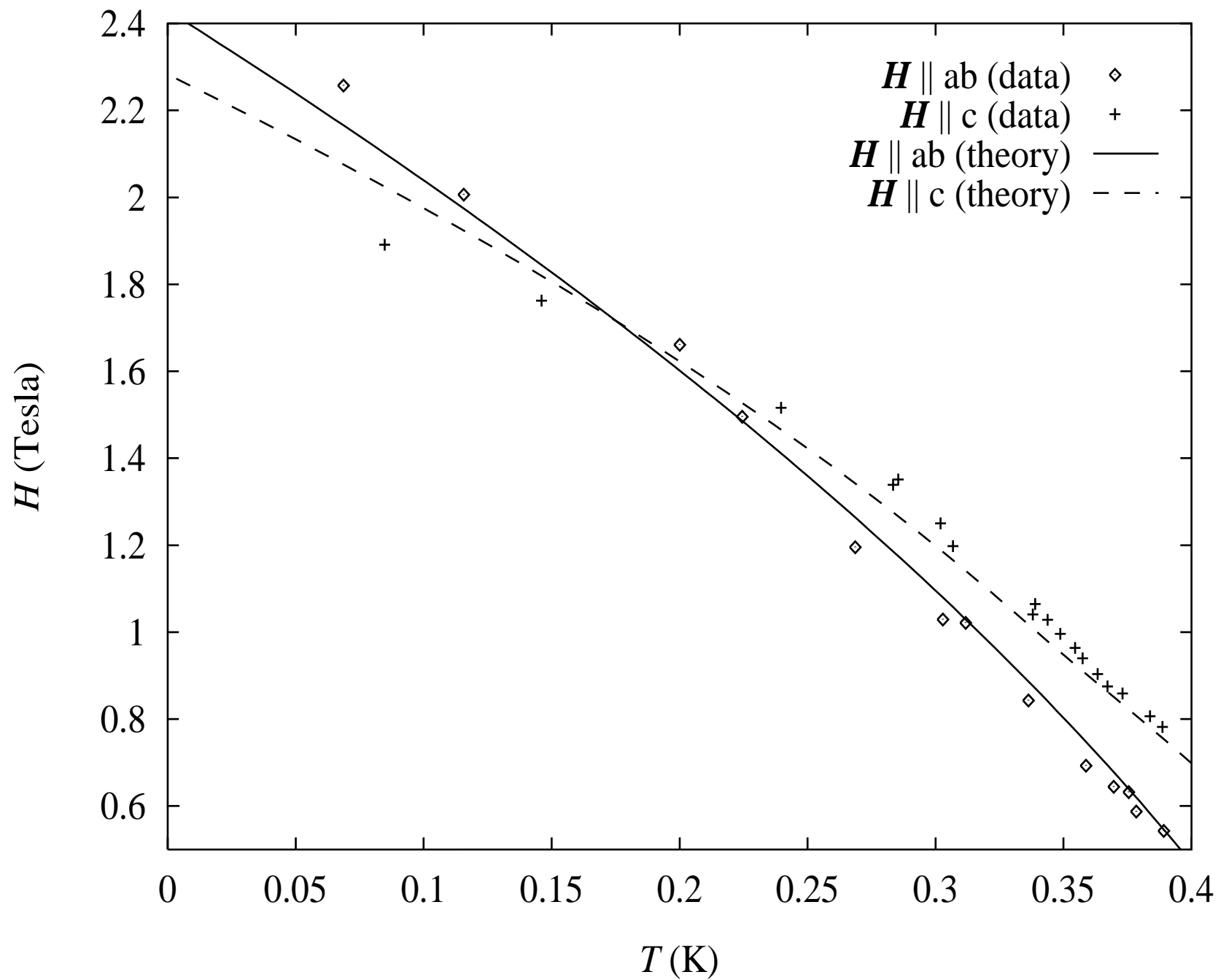
K. A. Park and Robert Joynt, Fig. 5



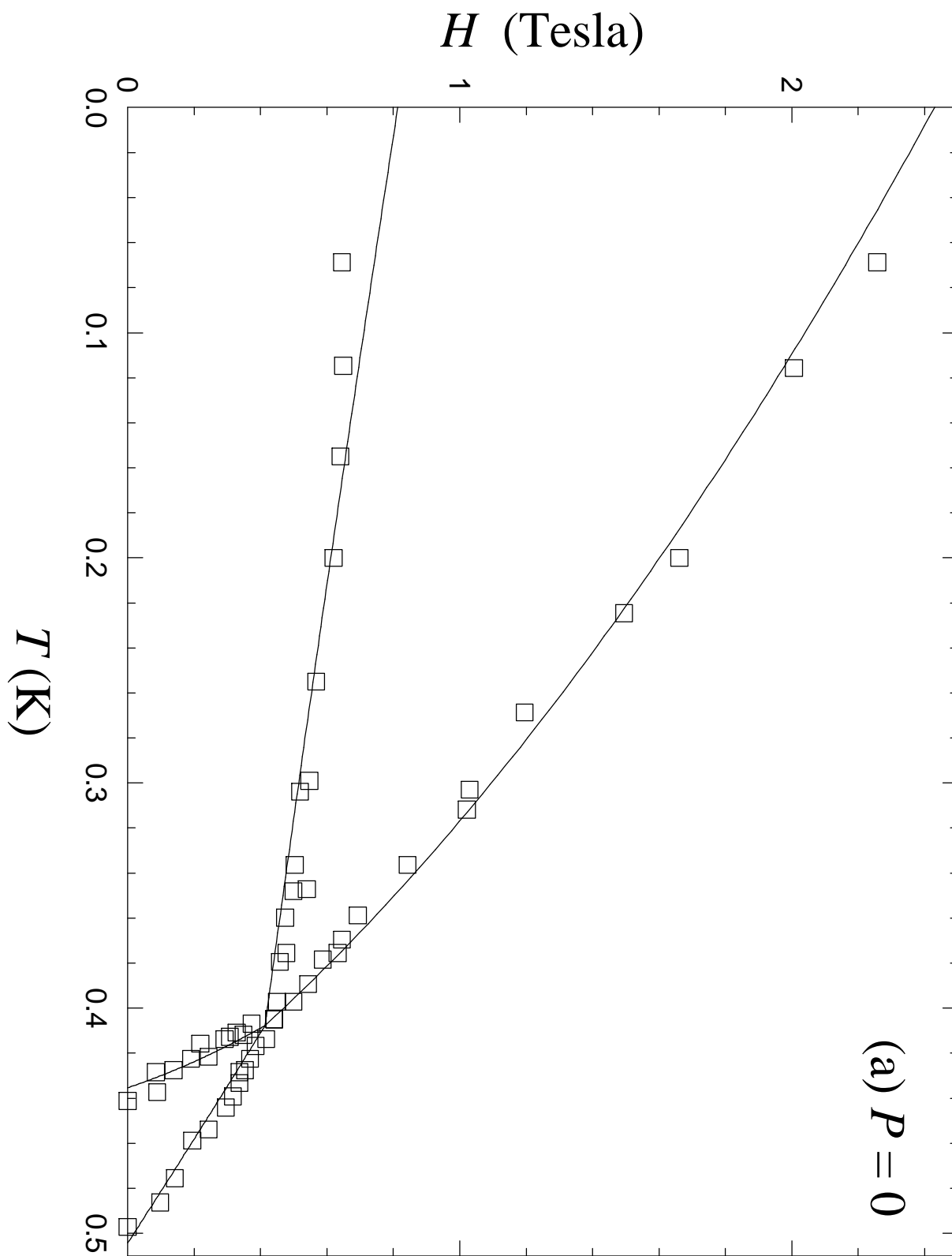
K. A. Park and Robert Joynt: Fig. 6



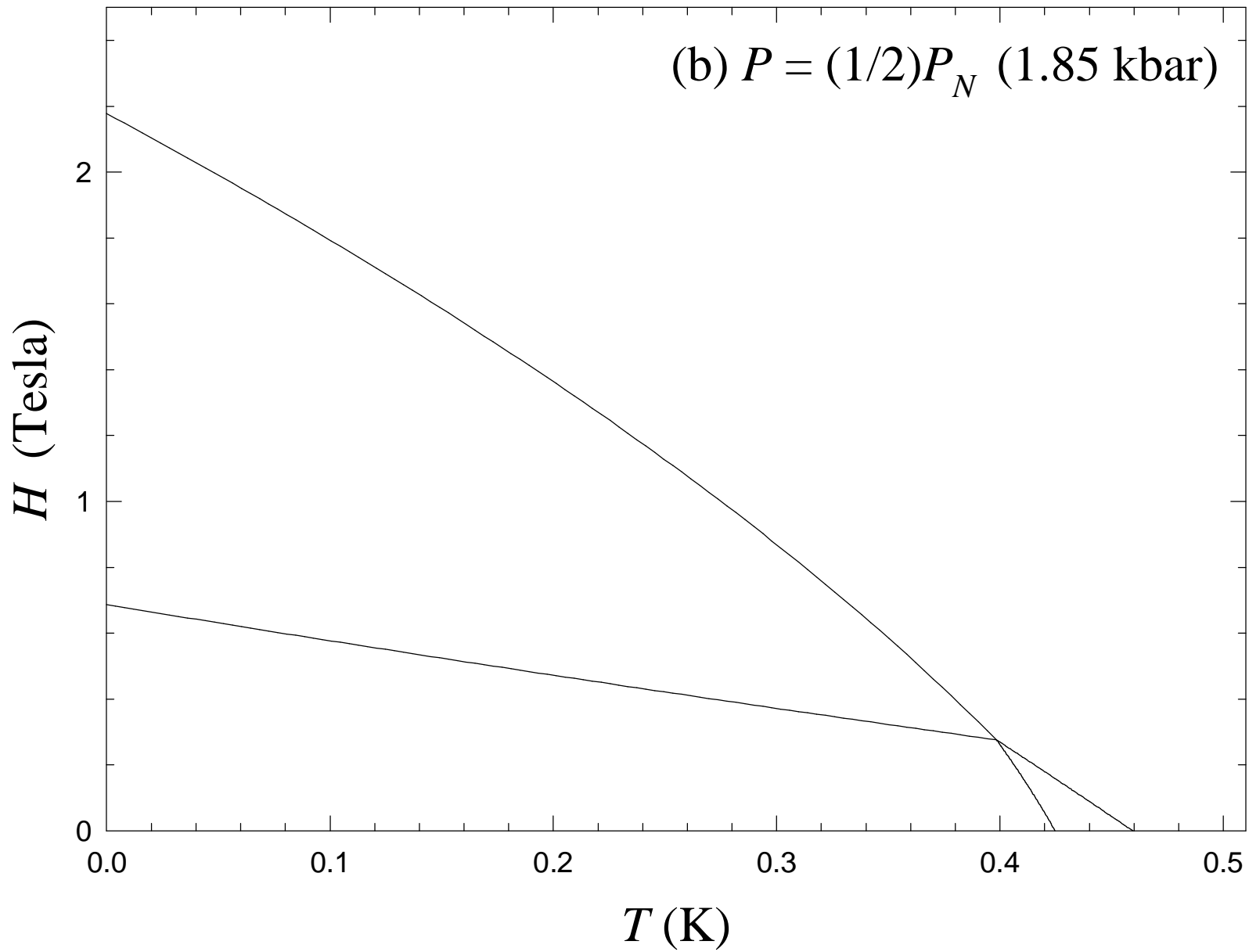
K. A. Park and Robert Joynt: Fig. 7



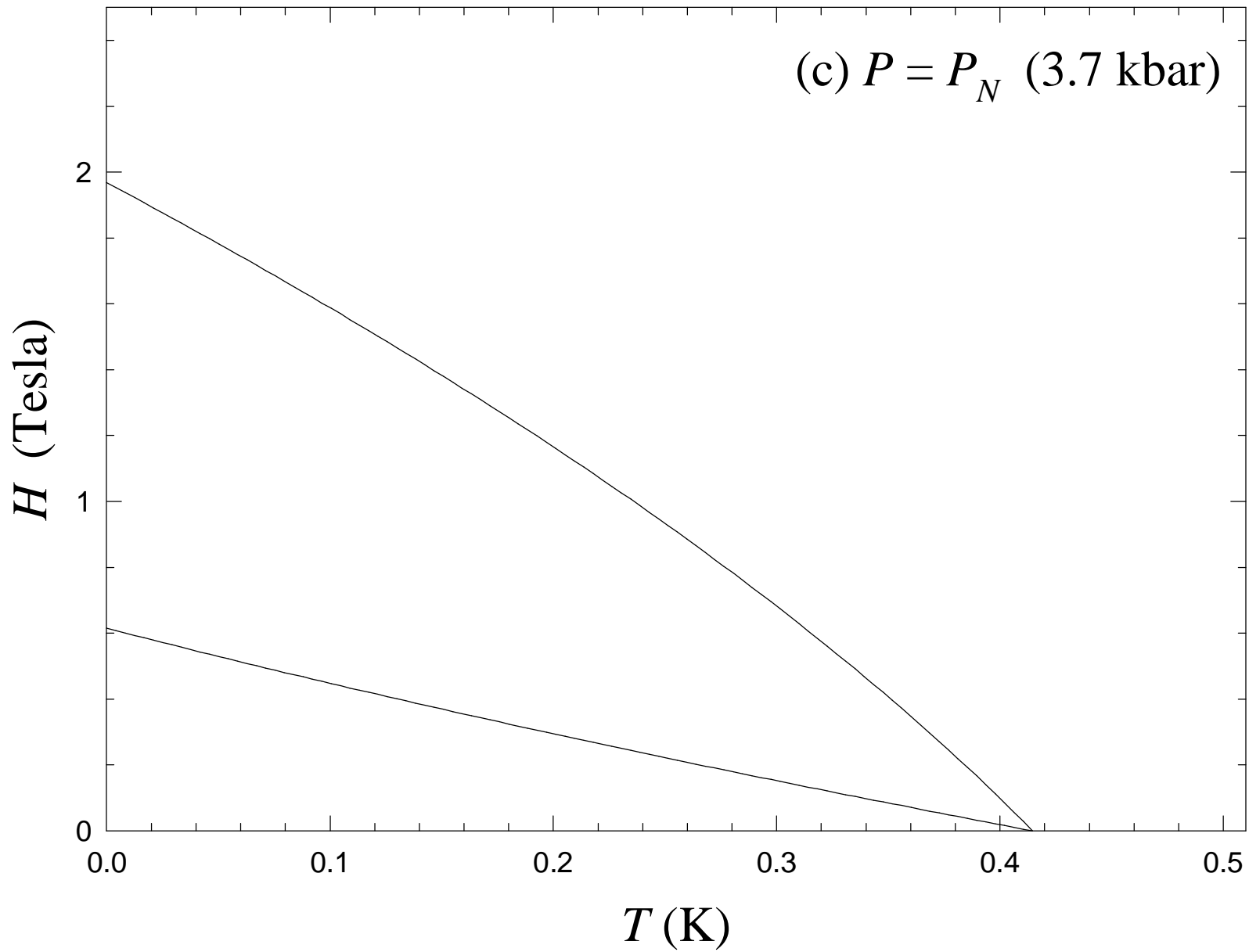
K. A. Park and Robert Joynt, Fig. 8



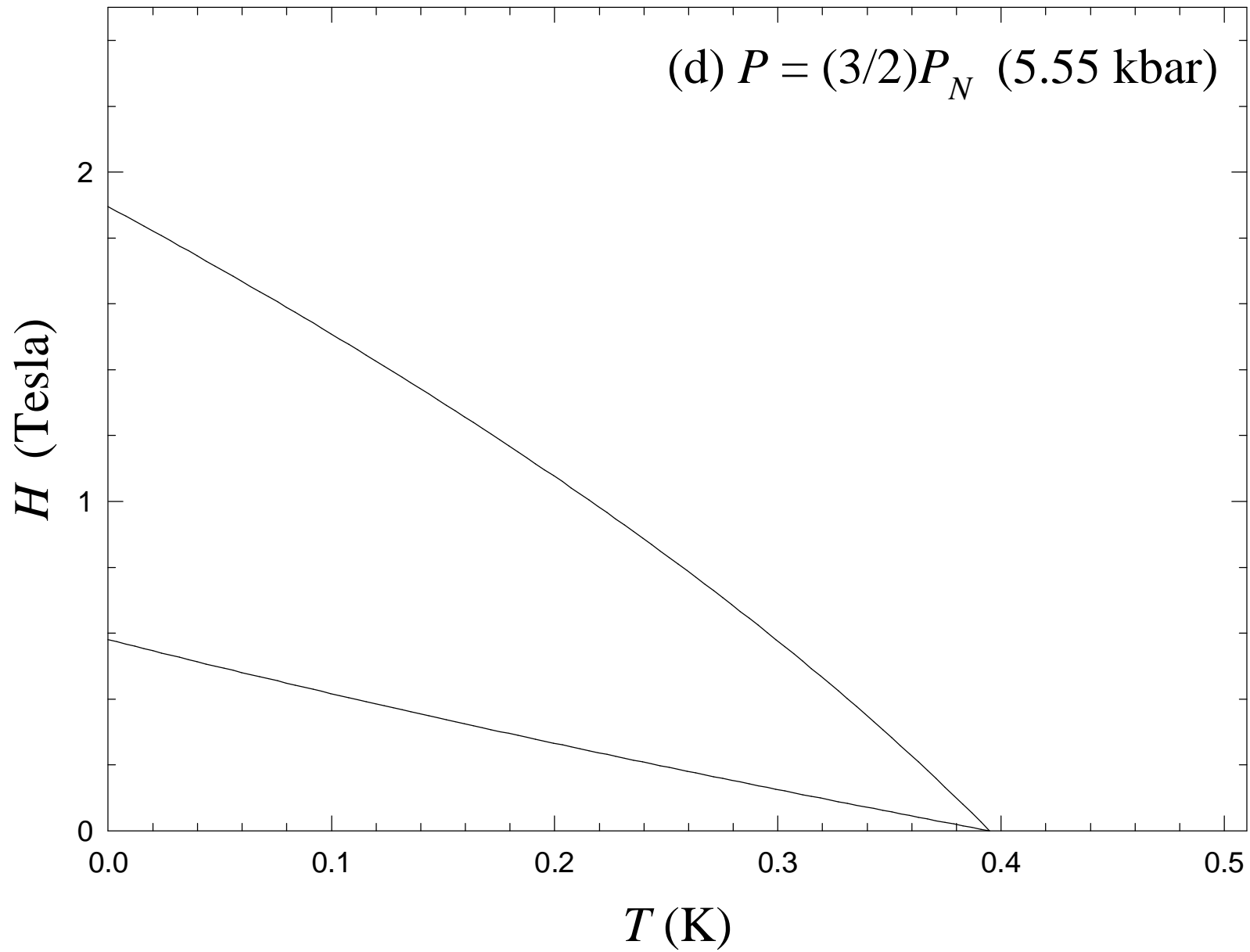
K. A. Park and Robert Joynt: Fig. 9(a)



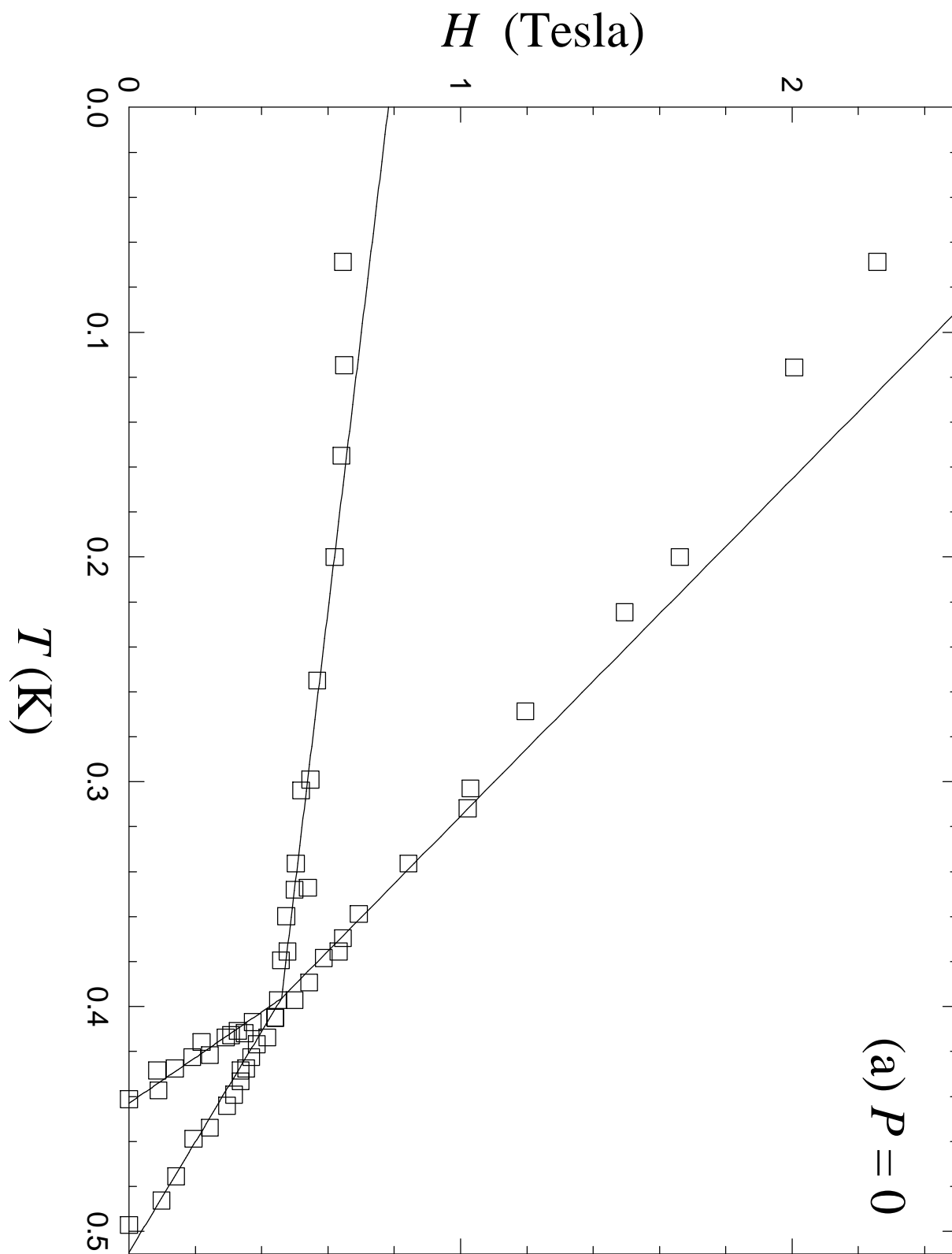
K. A. Park and Robert Joynt: Fig. 9(b)



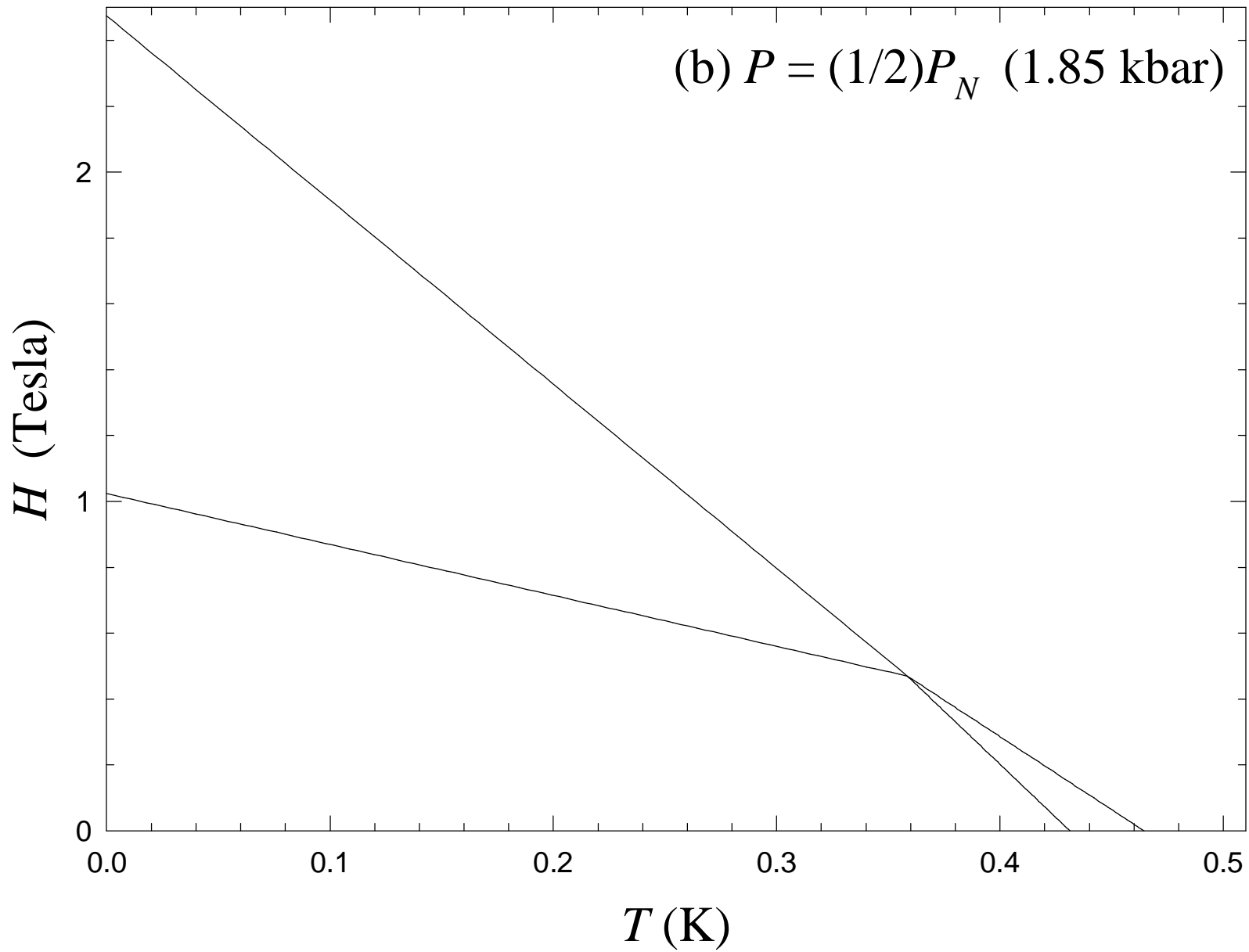
K. A. Park and Robert Joynt: Fig. 9(c)



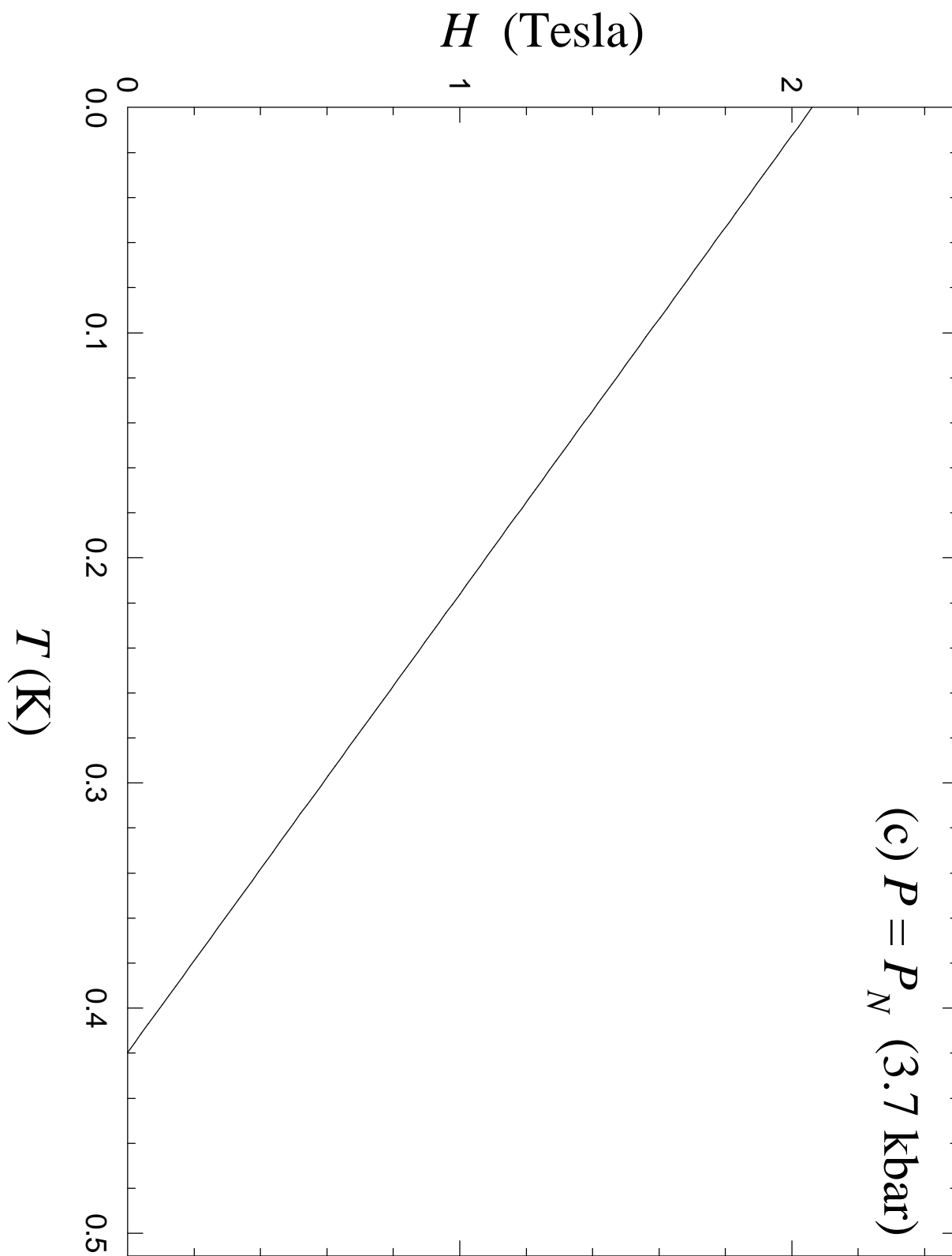
K. A. Park and Robert Joynt: Fig. 9(d)



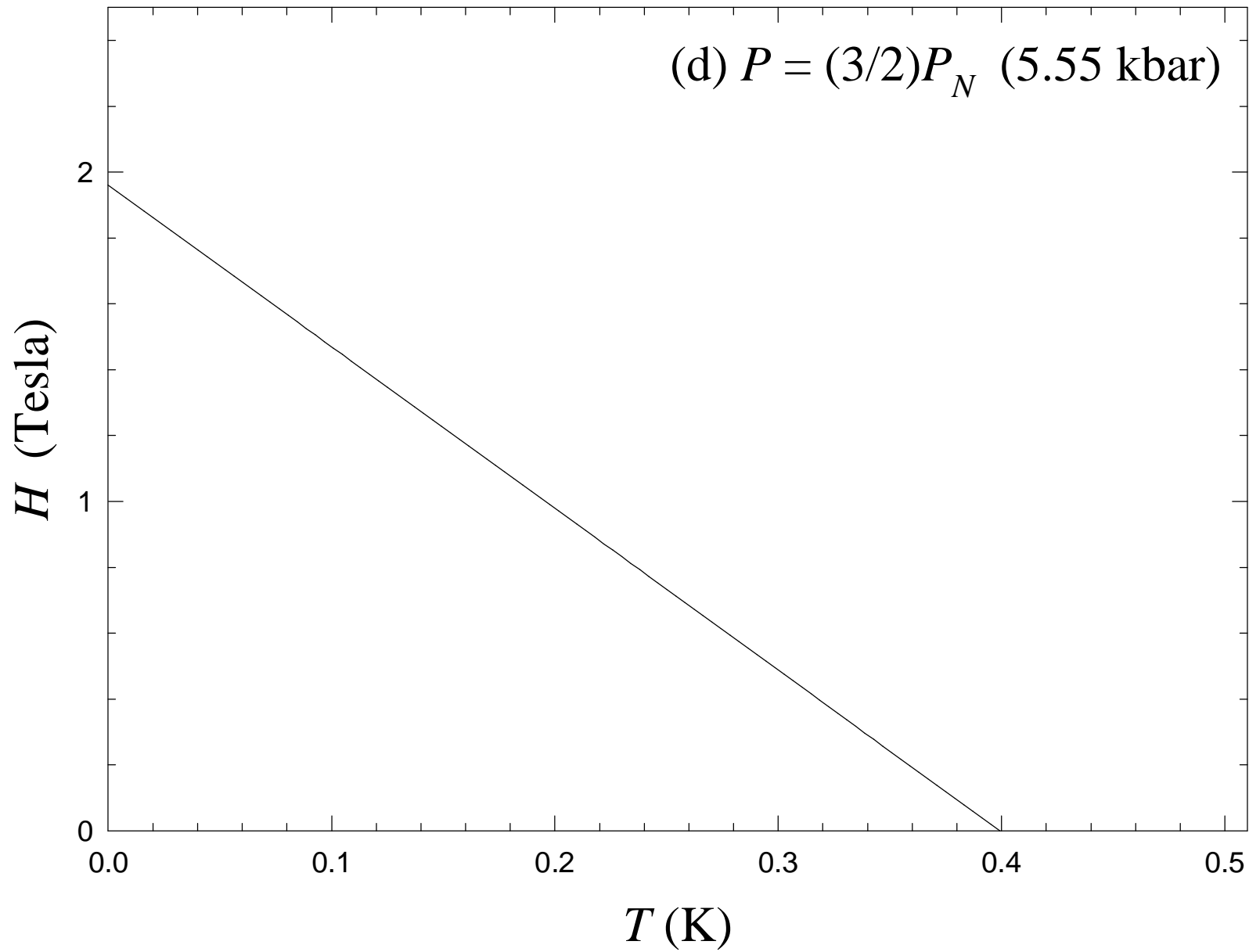
K. A. Park and Robert Joynt: Fig. 10(a)



K. A. Park and Robert Joynt: Fig. 10(b)



K. A. Park and Robert Joynt: Fig. 10(c)



K. A. Park and Robert Joynt: Fig. 10(d)